Supporting Information

Dielectric elastomer actuators with increased dielectric permittivity and low leakage current capable of overcoming electromechanical instability

Philip Caspari, Simon J. Dünki, Frank A. Nüesch, Dorina M. Opris*

P. Caspari, Dr. S. J. Dünki, Prof. F. Nüesch, Dr. D. M. Opris
Swiss Federal Laboratories for Materials Science and Technology Empa, Laboratory for Functional Polymers, Überlandstr. 129, CH-8600, Dübendorf, Switzerland
E-mail: dorina.opris@empa.ch
P. Caspari, Dr. S. J. Dünki, Prof. F. A. Nüesch
École Polytechnique Fédérale de Lausanne (EPFL), Institut des matériaux, Station 12, CH 1015, Lausanne, Switzerland

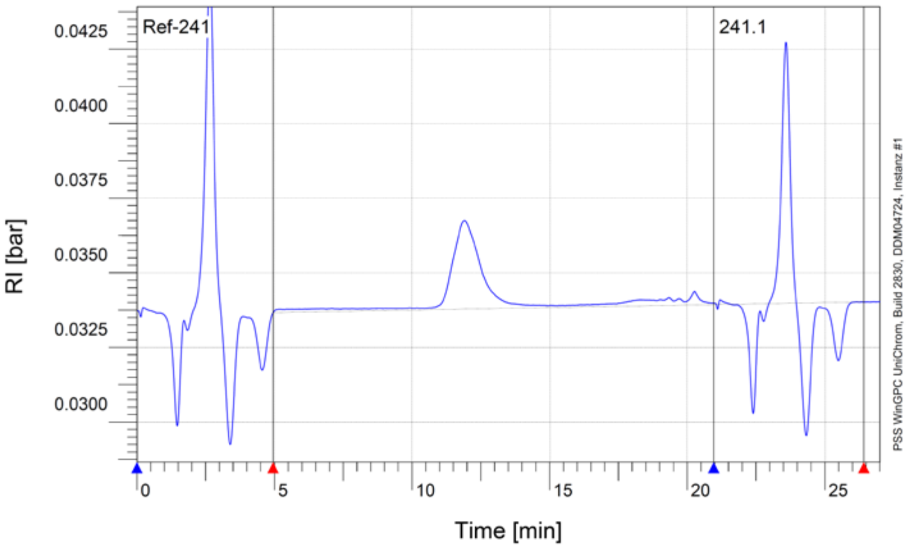

Probe :	Ref-241	**Methode :**	C:\EmpaDaten\Methoden\TFE_Fischer_01_2014.
Basislinie von :	4.950 ml	**bis :**	26.417 ml
Integration von :	4.917 ml	**bis :**	26.242 ml
Kalibration :	PDMS_THF_alteSäule_31012014.cal	**Eluent :**	THF
MHK - A (Kal.):	0.000E+0	**MHK - K (Kal.):**	1.000E+0 ml/g
Int.Stand.-K :	23.429 ml	**Int.Stand.-M :**	23.585 ml
Pumpe :	PSS SECcurity	**Flußrate :**	1.000 ml/min
Konzentration :	2.000 g/l	**Injektvolumen :**	20.000 ul
Säule 1 :	PSS SDV 5µm	**Temperatur :**	30.000 °C
Säule 2 :	PSS SDV 5µm	**Temperatur :**	30.000 °C
Detektor 1 :	PSS SECcurity UV	**Versatz :**	0.000 ml
Detektor 2 :	PSS SECcurity UV	**Versatz :**	0.160 ml
Detektor 3 :	PSS SECcurity RI	**Versatz :**	0.000 ml
Operateur :	Beatrice Fischer	**Messintervall :**	1.000 sec

Figure S1. GPC elution curve of **P0**.

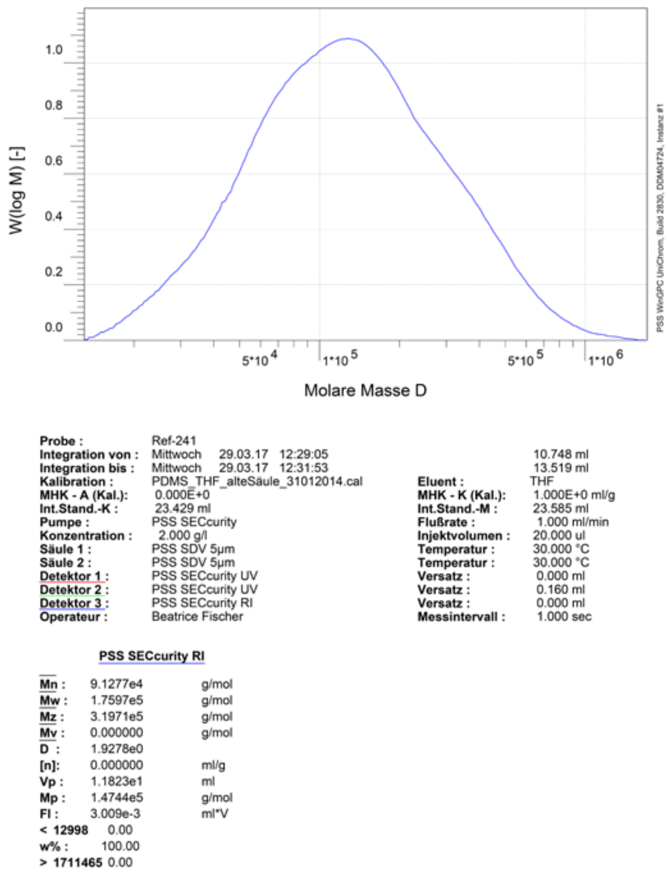

Figure S2. GPC analysis of **P0** (M_n = 90.000 g mol^{-1}, M_w = 175.000 g mol^{-1}, PDI = 1.9).

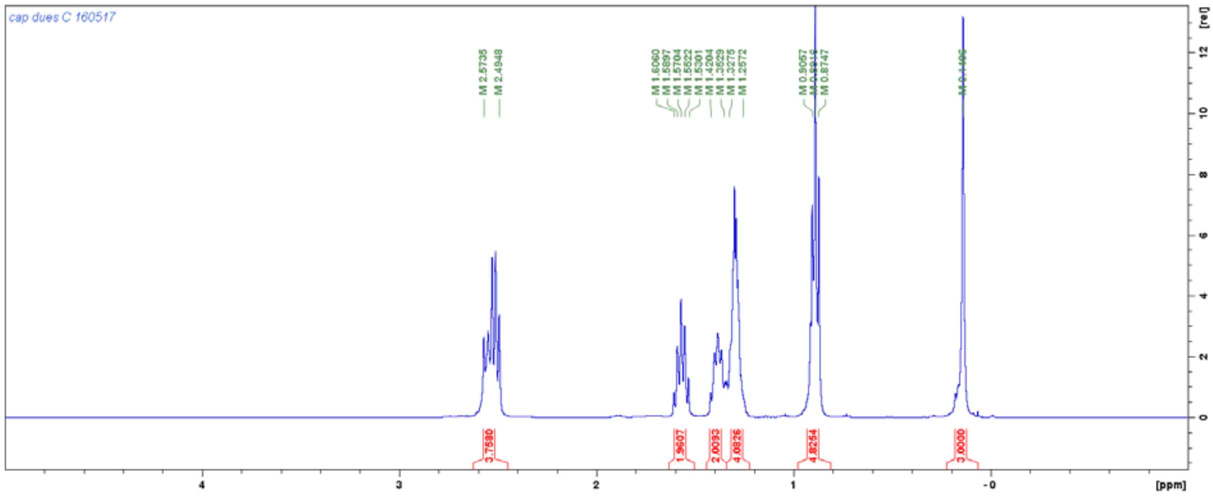

Figure S3. [1]H NMR spectrum of **P2**.

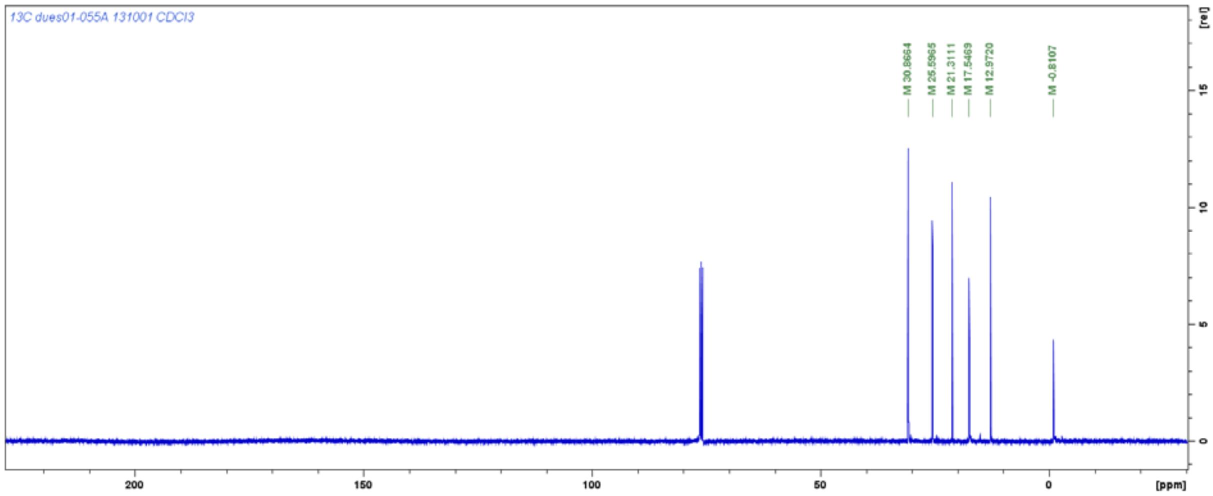

Figure S4. ^{13}C NMR spectrum of **P2**.

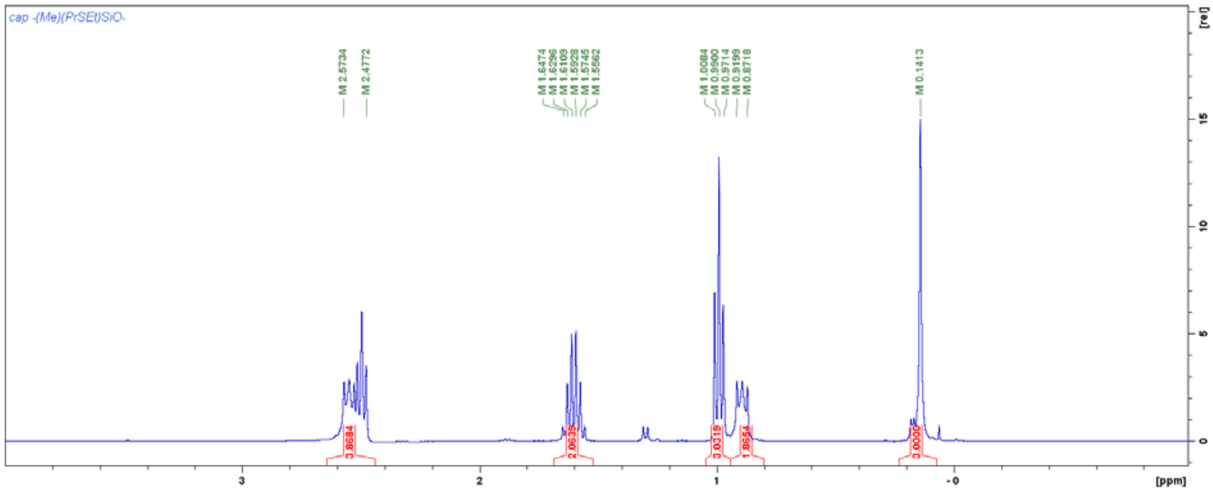

Figure S5. ^{1}H NMR spectrum of **P3**.

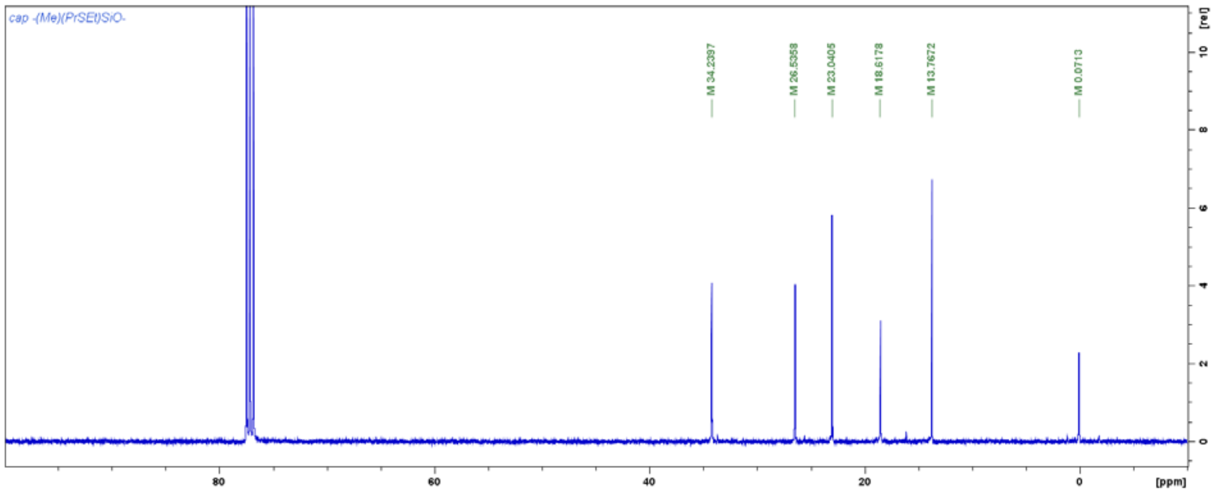

Figure S6. ^{13}C NMR spectrum of **P3**.

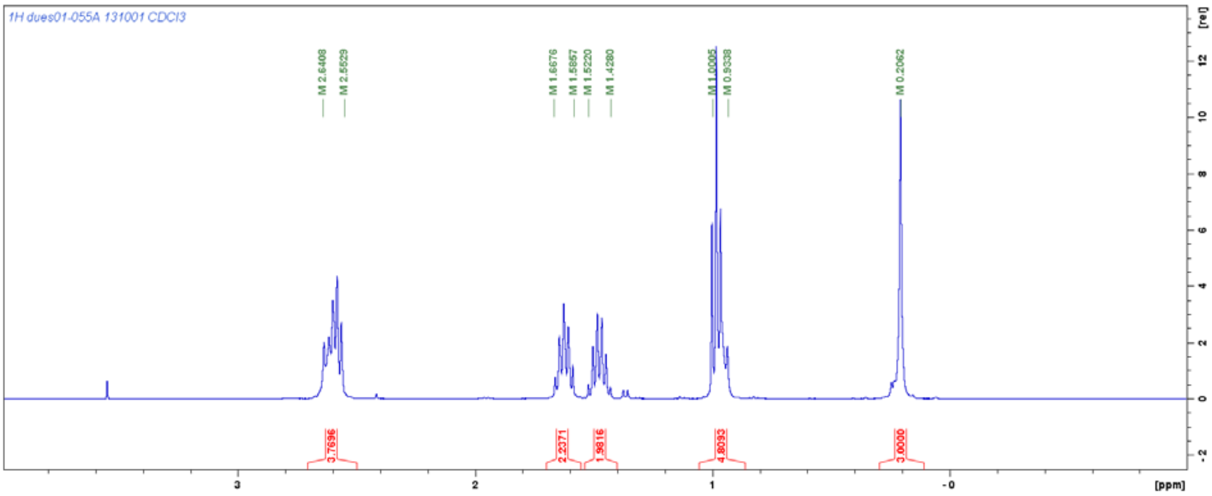

Figure S7. ^{1}H NMR spectrum of **P4**.

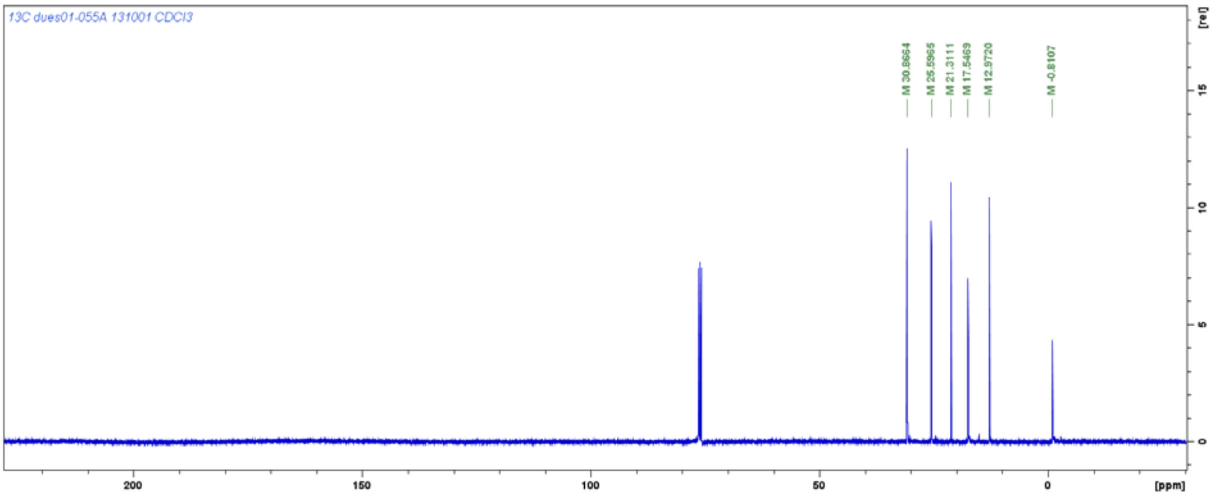

Figure S8. ^{13}C NMR spectrum of **P4**.

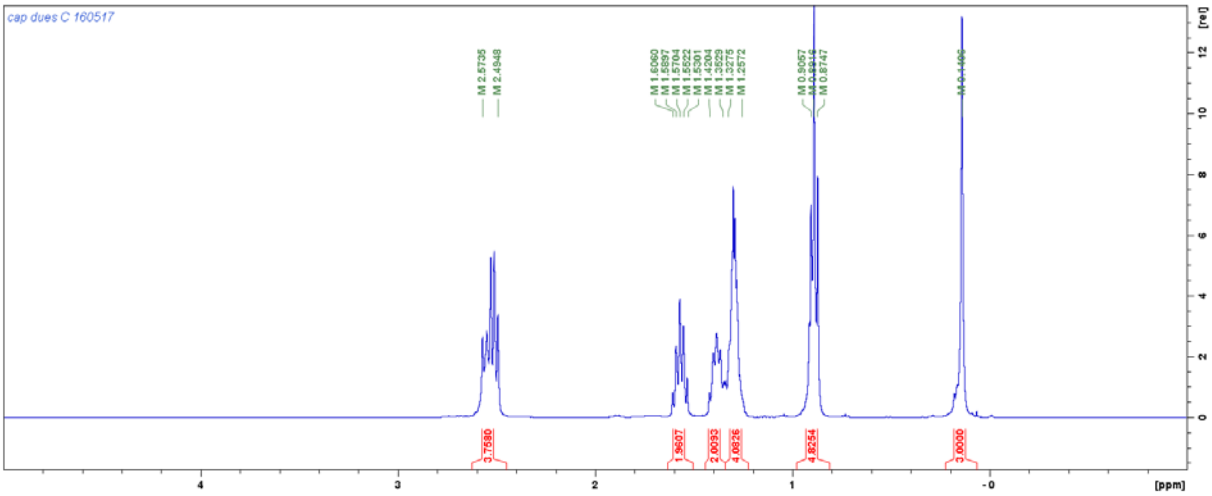

Figure S9. ^{1}H NMR spectrum of **P6**.

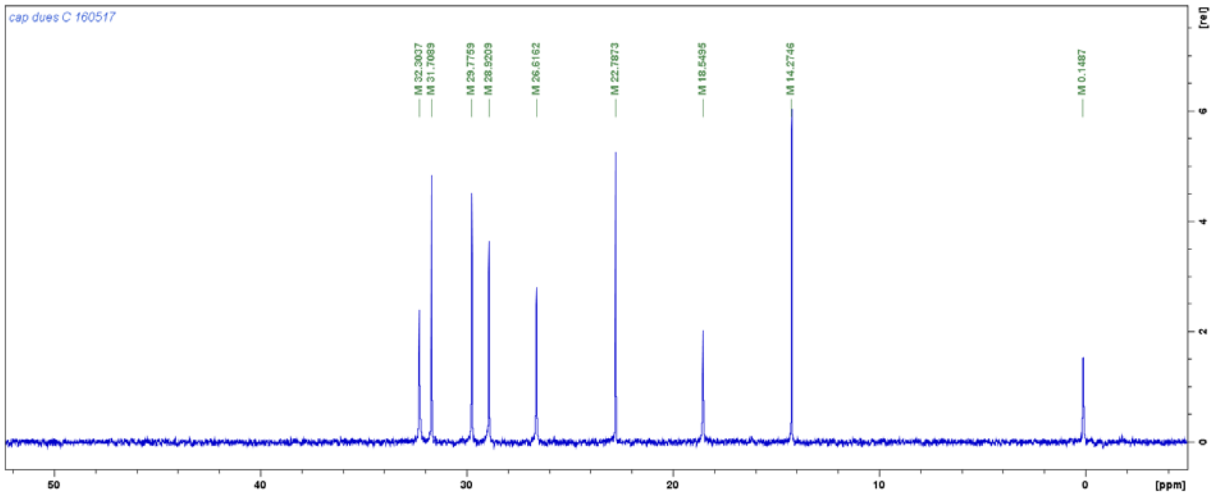

Figure S10. ^{13}C NMR spectrum of **P6**.

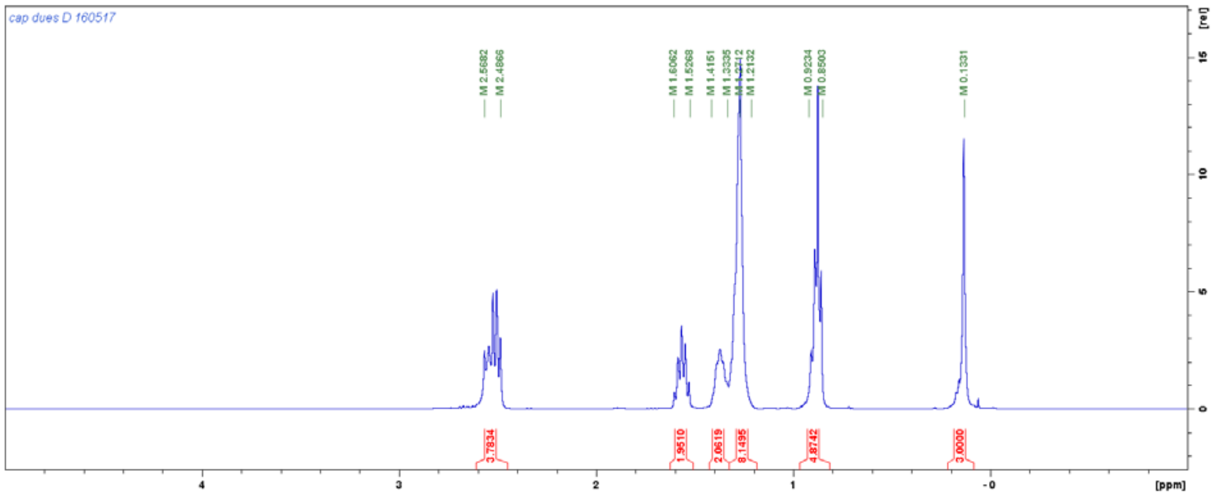

Figure S11. ^{1}H NMR spectrum of **P8**.

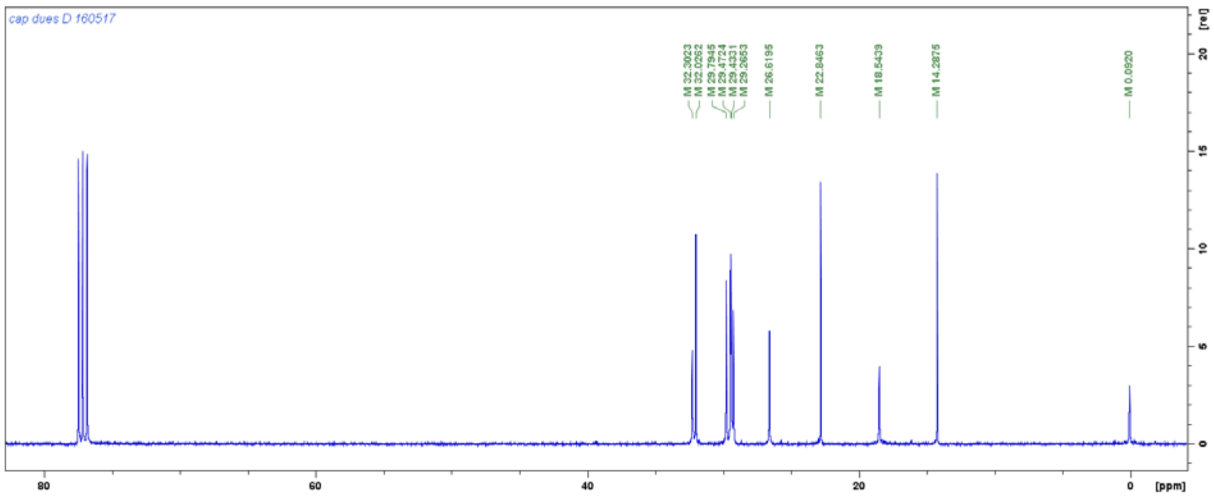

Figure S12. ^{13}C NMR spectrum of **P8**.

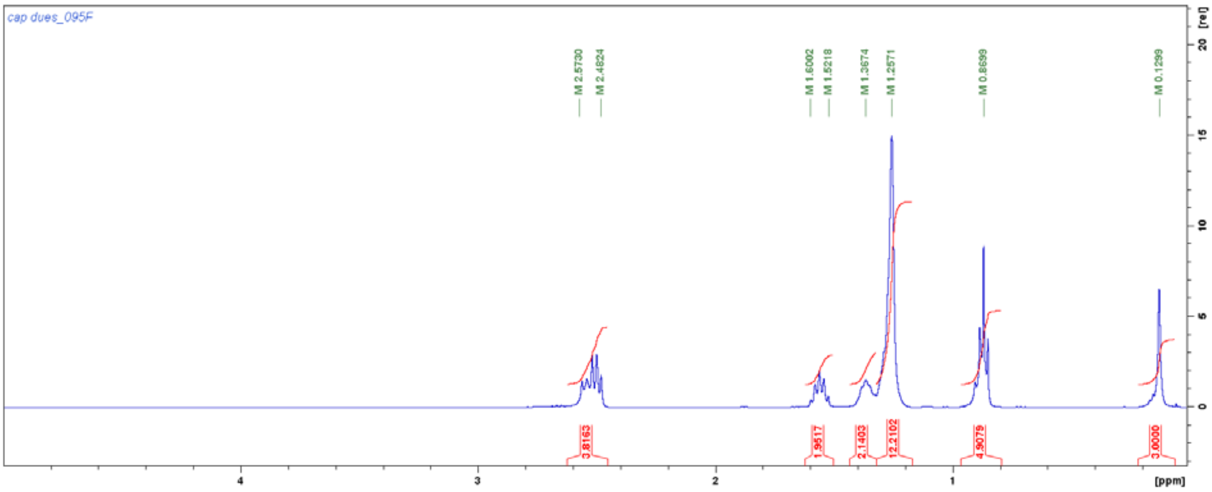

Figure S13. ^{1}H NMR spectrum of **P10**.

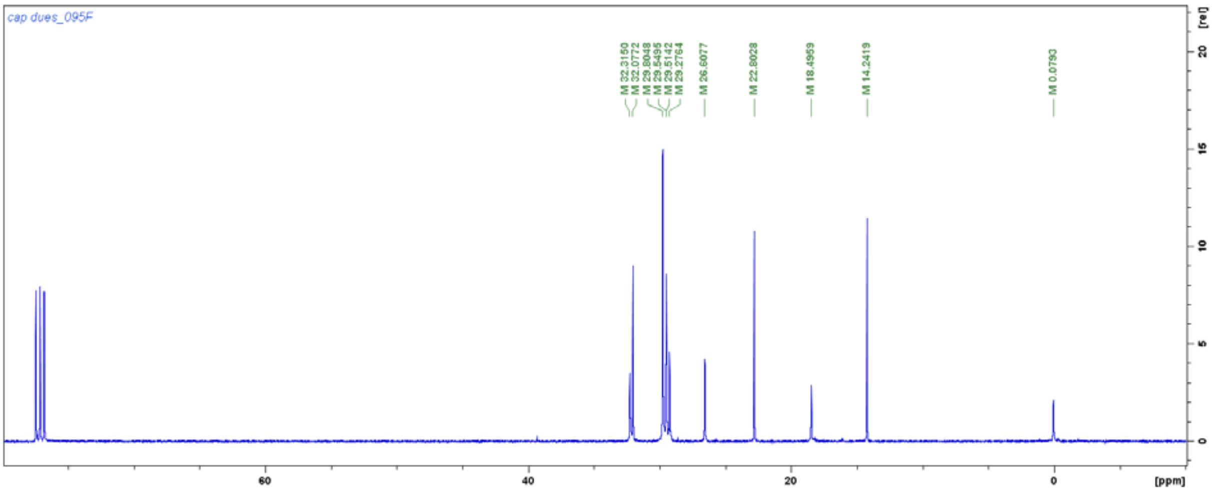

Figure S14. ^{13}C NMR spectrum of **P10**.

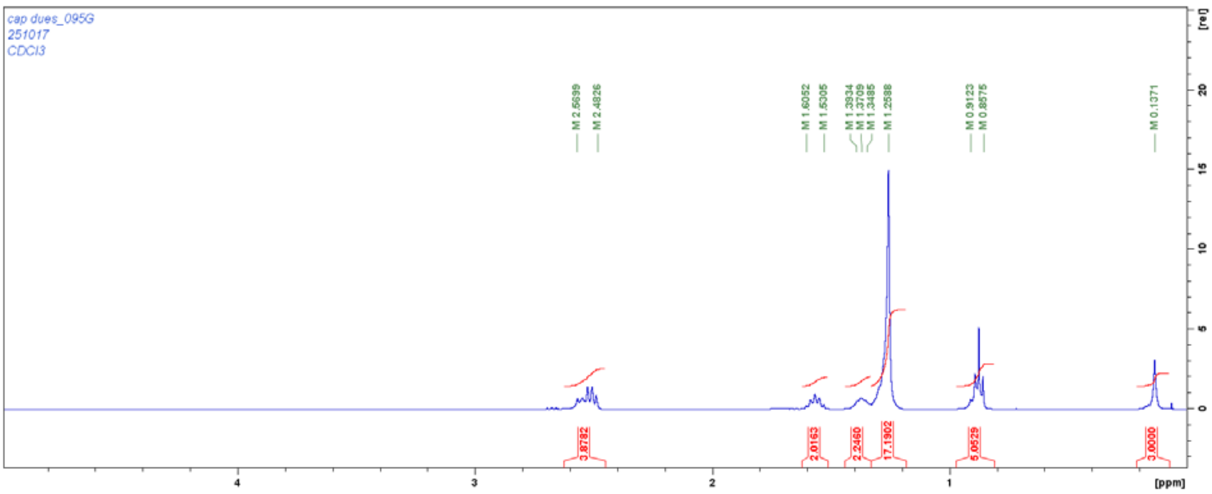

Figure S15. ^{1}H NMR spectrum of **P12**.

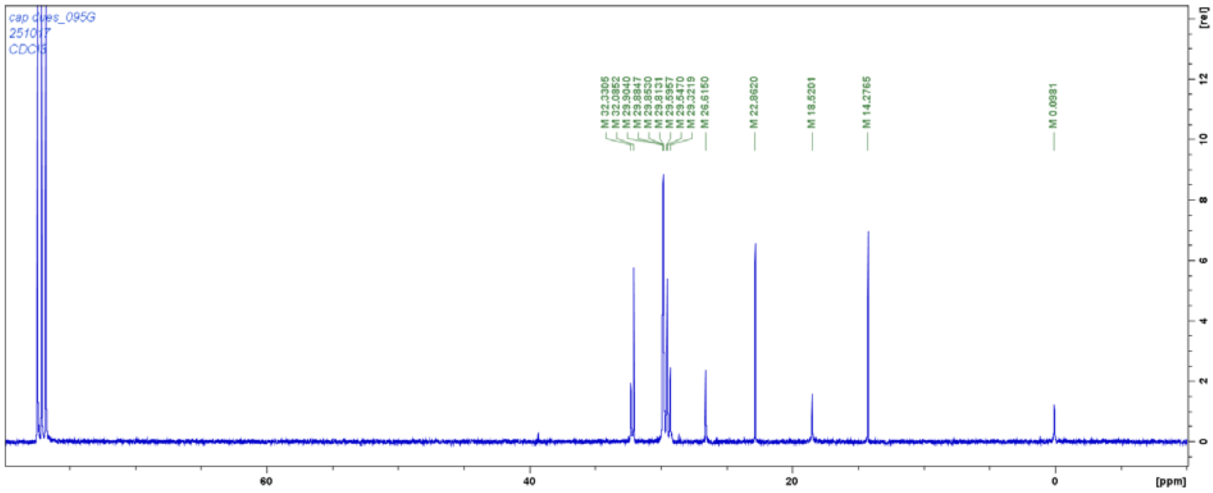

Figure S16. ^{13}C NMR spectrum of **P12.**

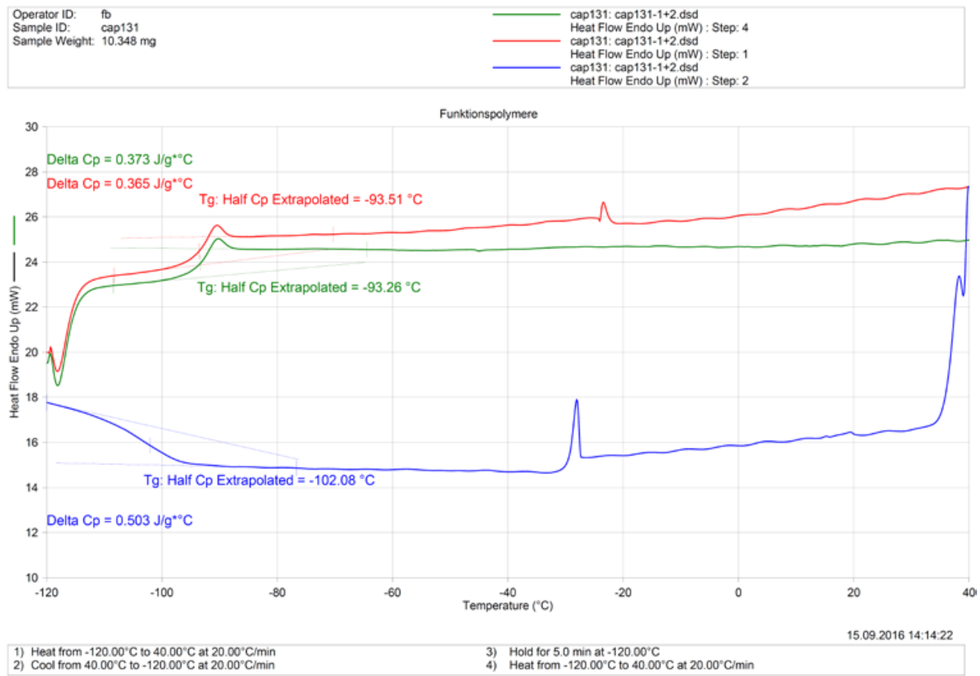

Figure S17. DSC curves of **P2**.

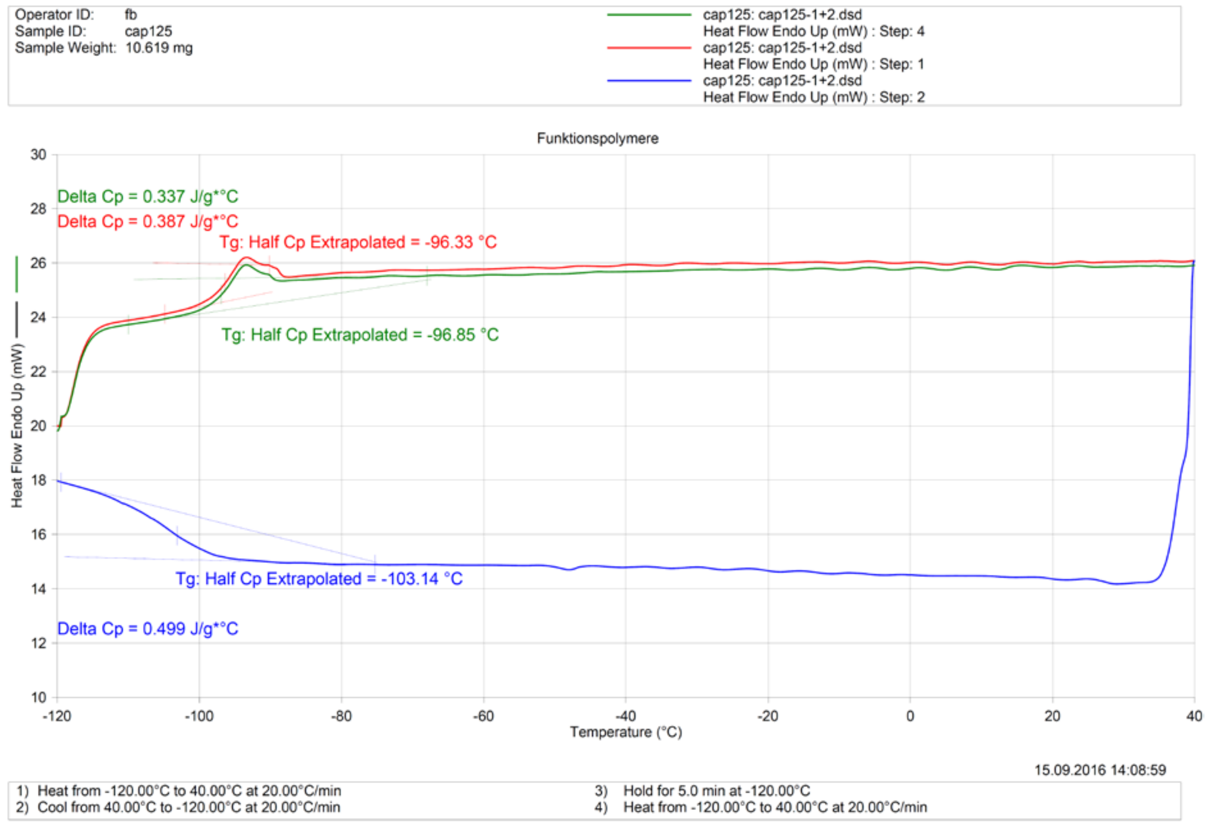

Figure S18. DSC curves of **P2**.

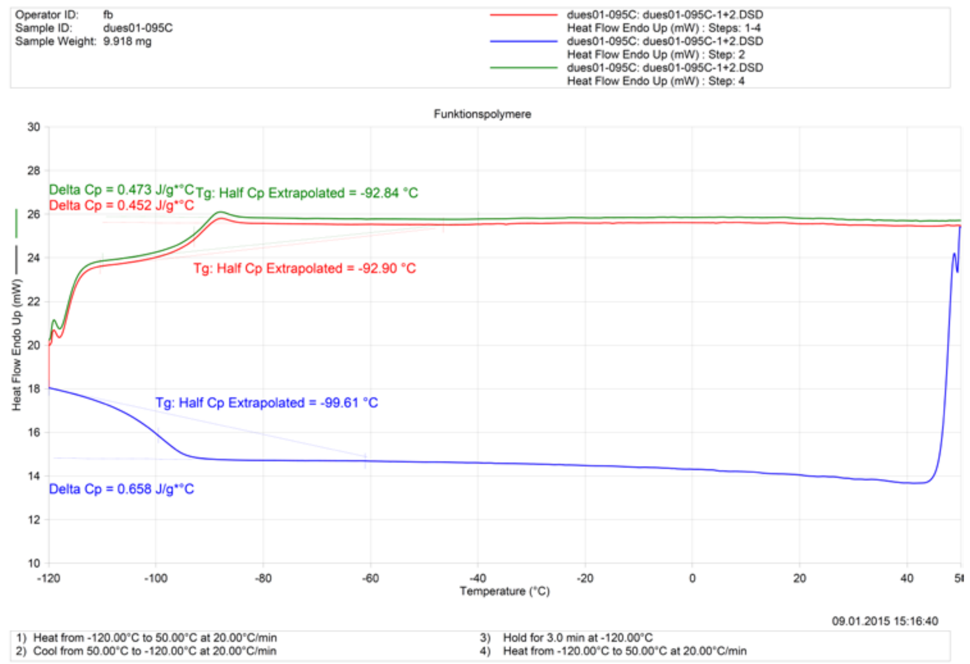

Figure S19. DSC curves of **P6**.

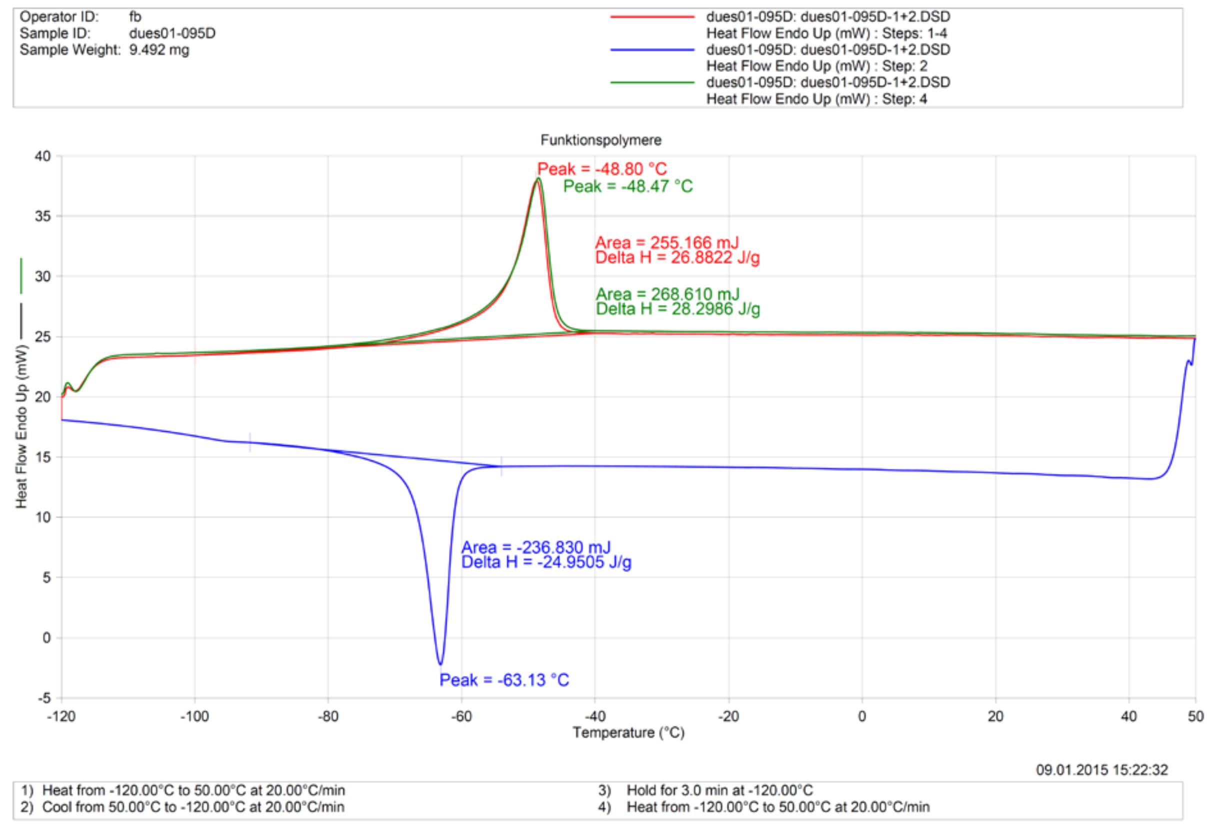

Figure S20. DSC curves of **P8**.

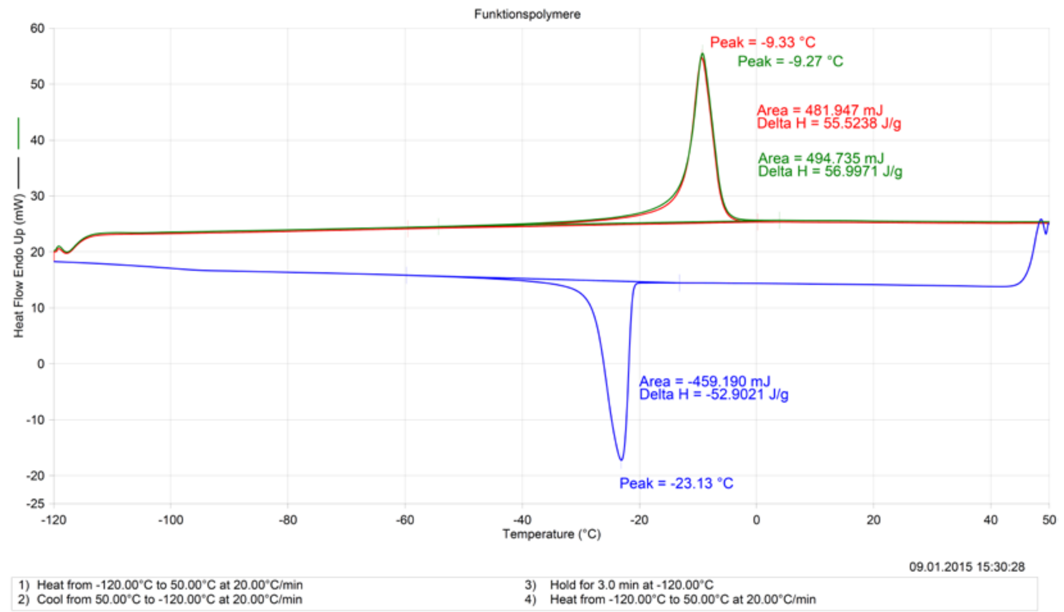

Figure S21. DSC curves of **C10**.

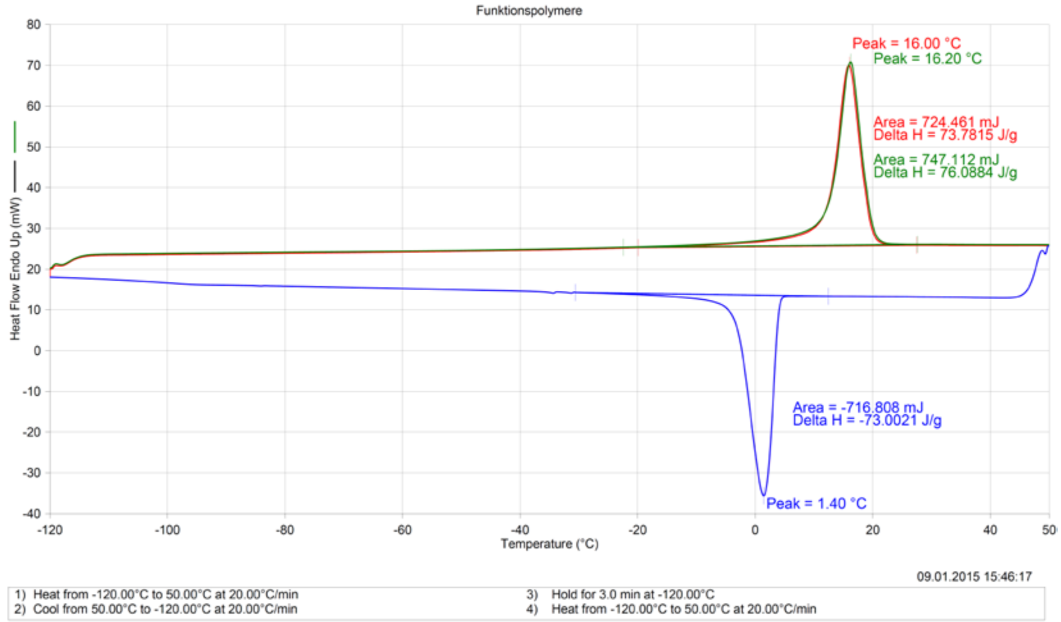

Figure S22. DSC curves of **P12**.

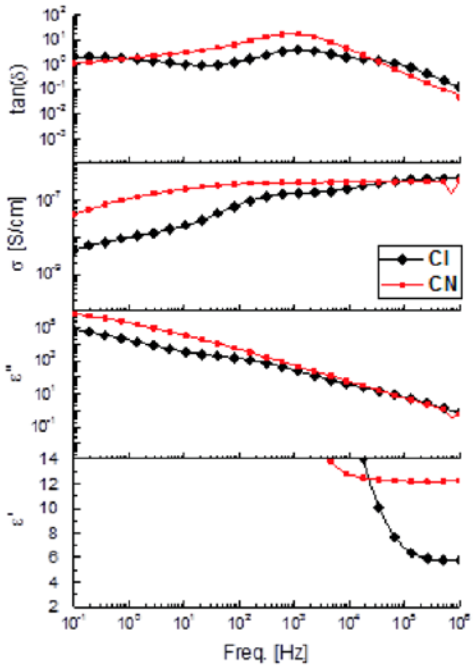

Figure **S23**. Dielectric properties of Cl-CL and CN-CL. Dielectric permittivity ε' was taken at 10^6 Hz where the contribution of ions can be neglected.

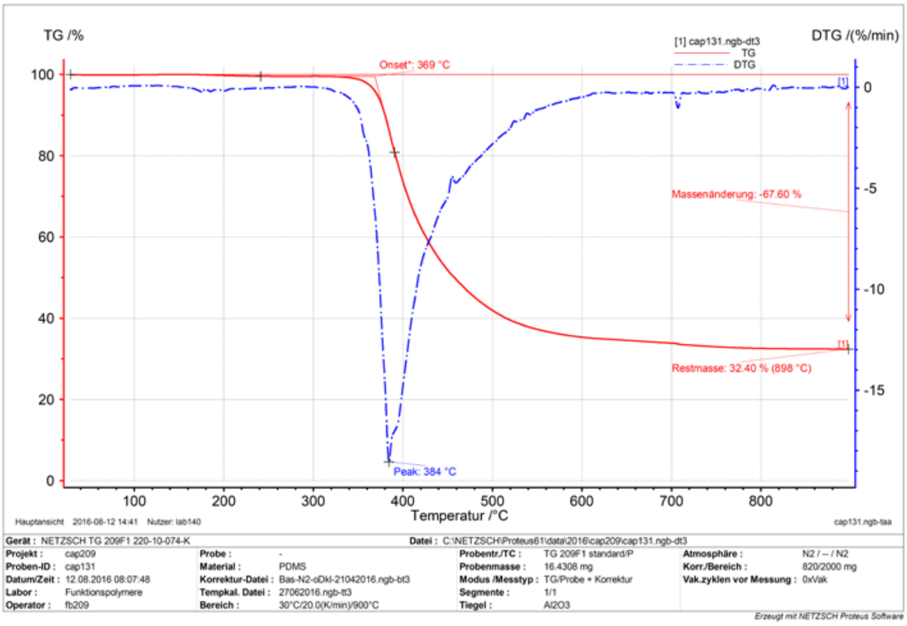

Figure S24. TGA curve of **P2**.

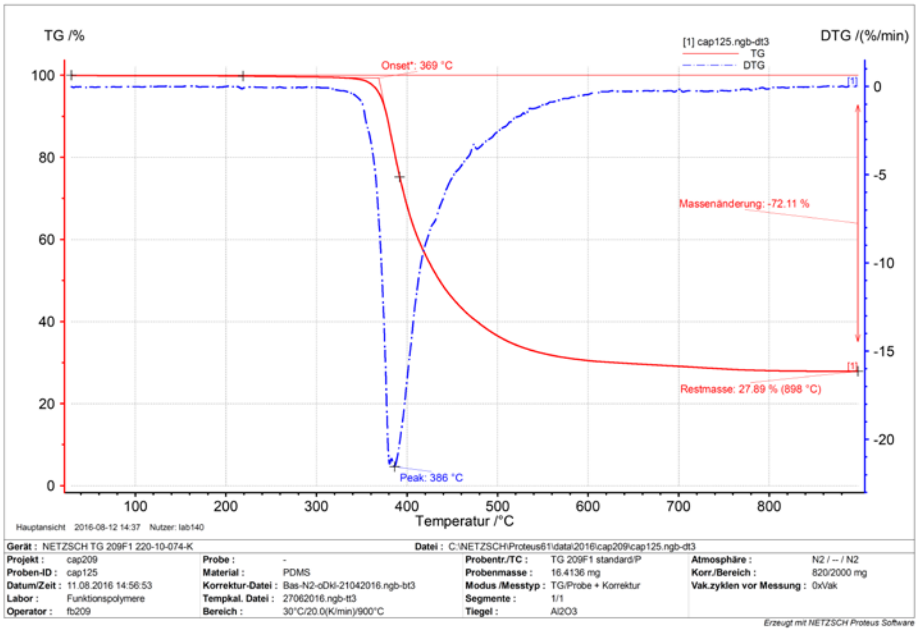

Figure S25. TGA curve of **P3**.

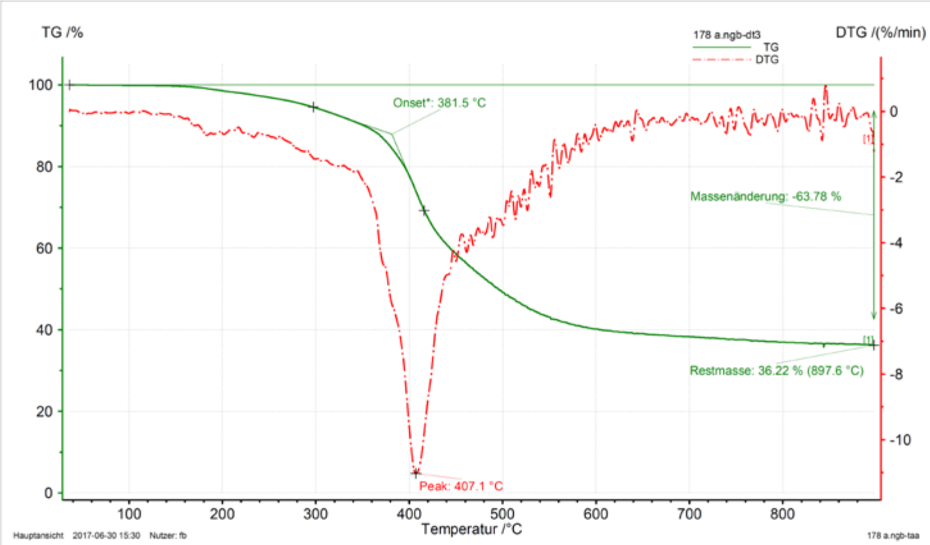

Figure S26. TGA curve of **E2-Cl-33**.

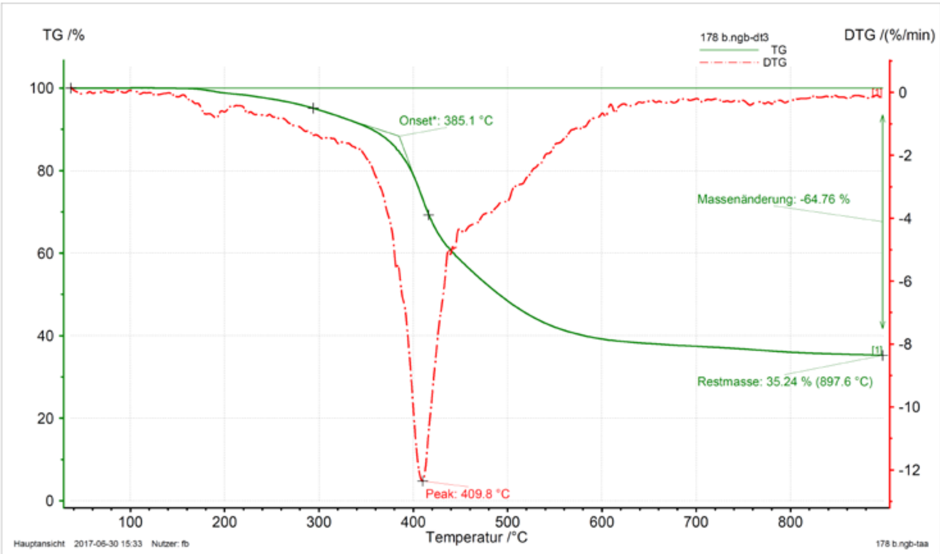

Figure S27. TGA curve of **E2-Cl-20**.

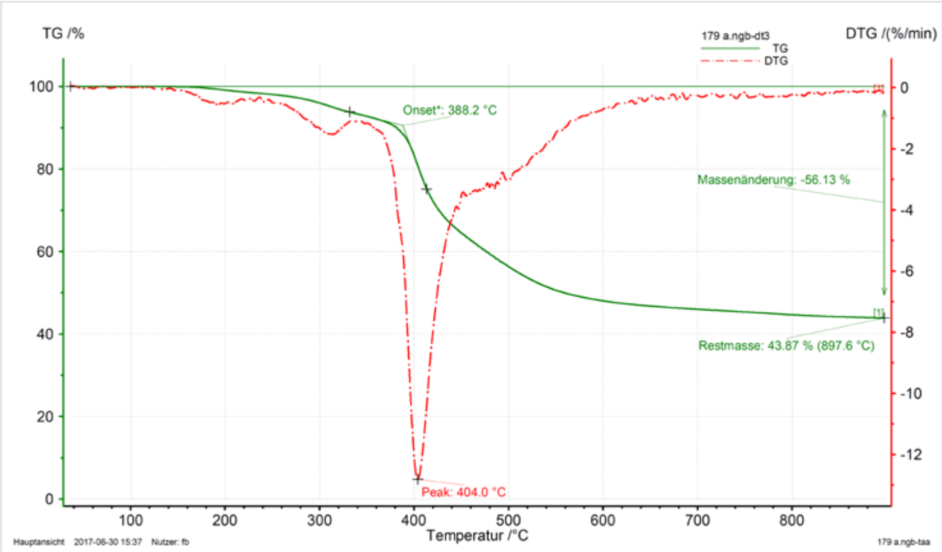

Figure S28. TGA curve of **E2-CN-33**.

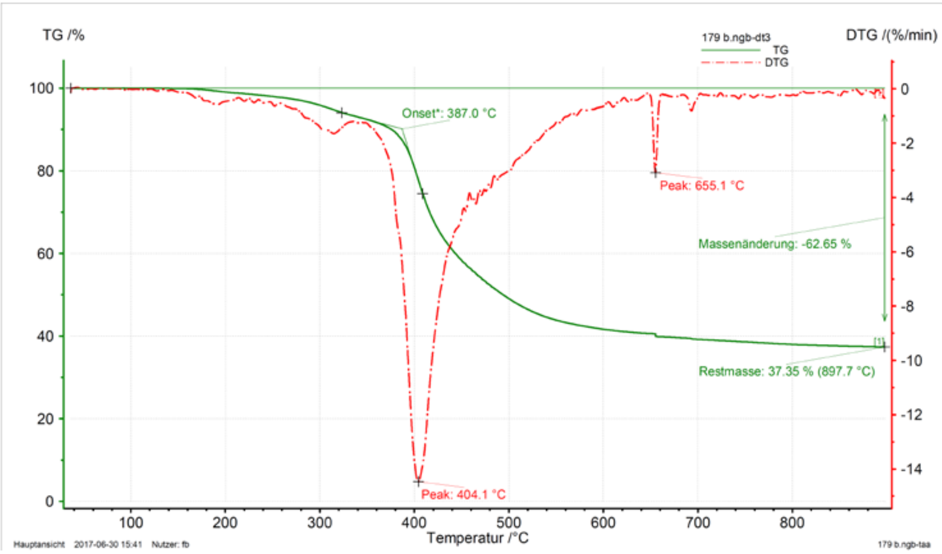

Figure S29. TGA curve of **E2-CN-20**.

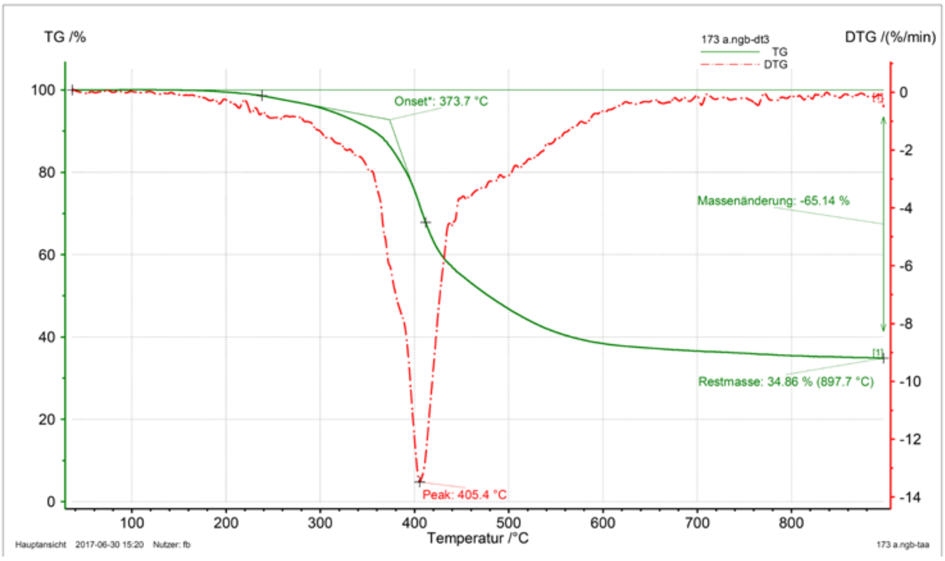

Figure S30. TGA curve of **E3-Cl-33**.

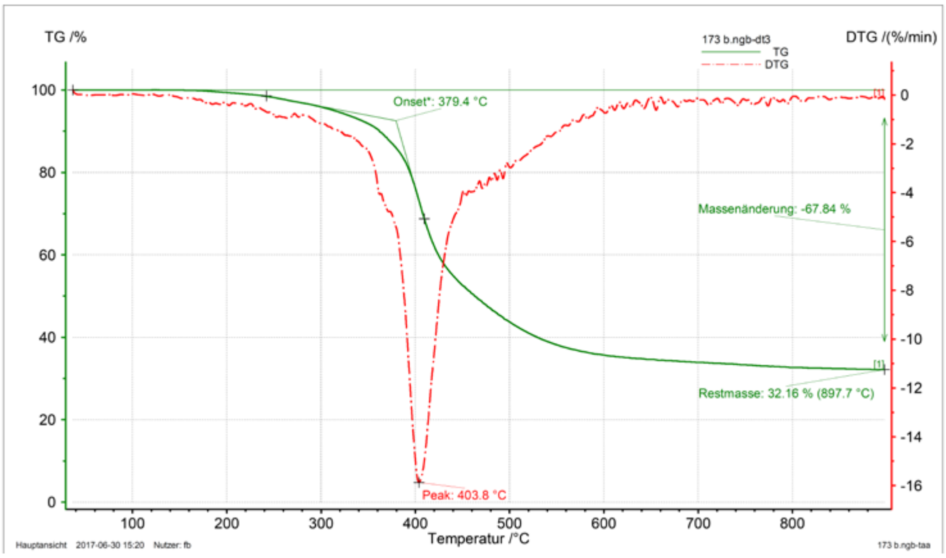

Figure S31. TGA curve of **E3-Cl-20**.

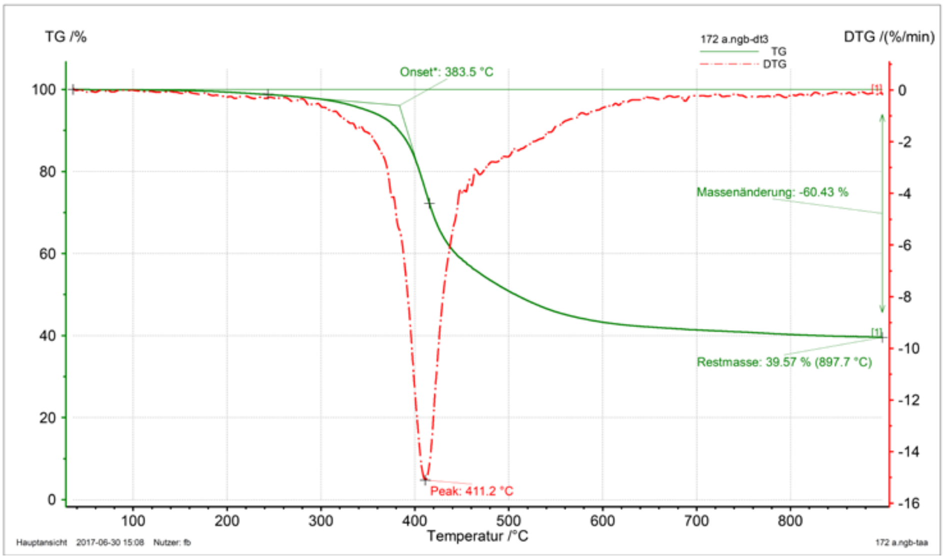

Figure S32. TGA curve of **E3-CN-33**.

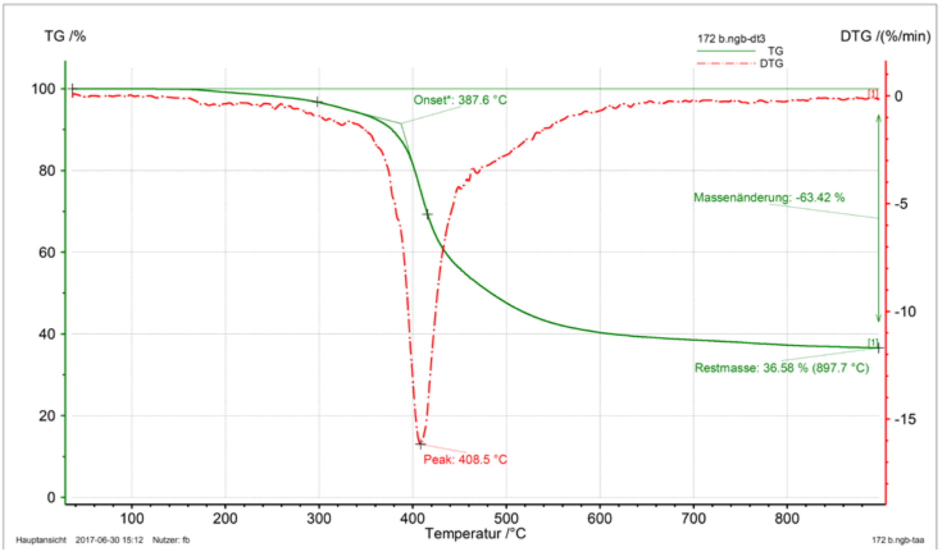

Figure S33. TGA curve of **E3-CN-20**.

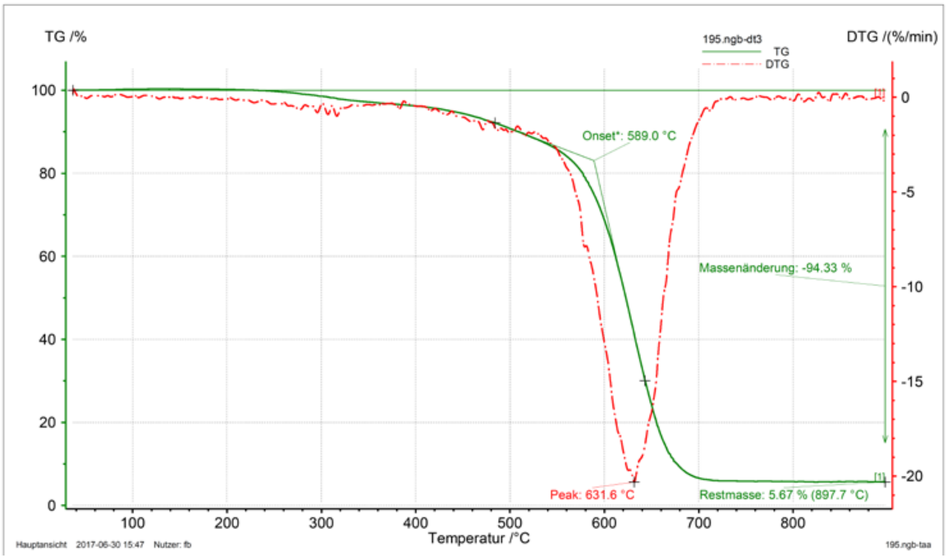

Figure S34. TGA curve of **Er-Cl-33**.

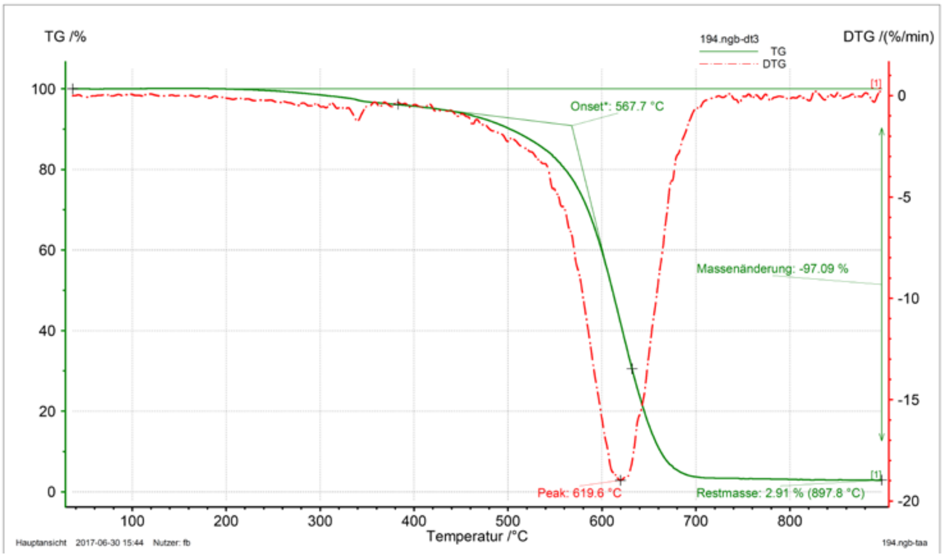

Figure S35. TGA curve of **Er-Cl-20**.

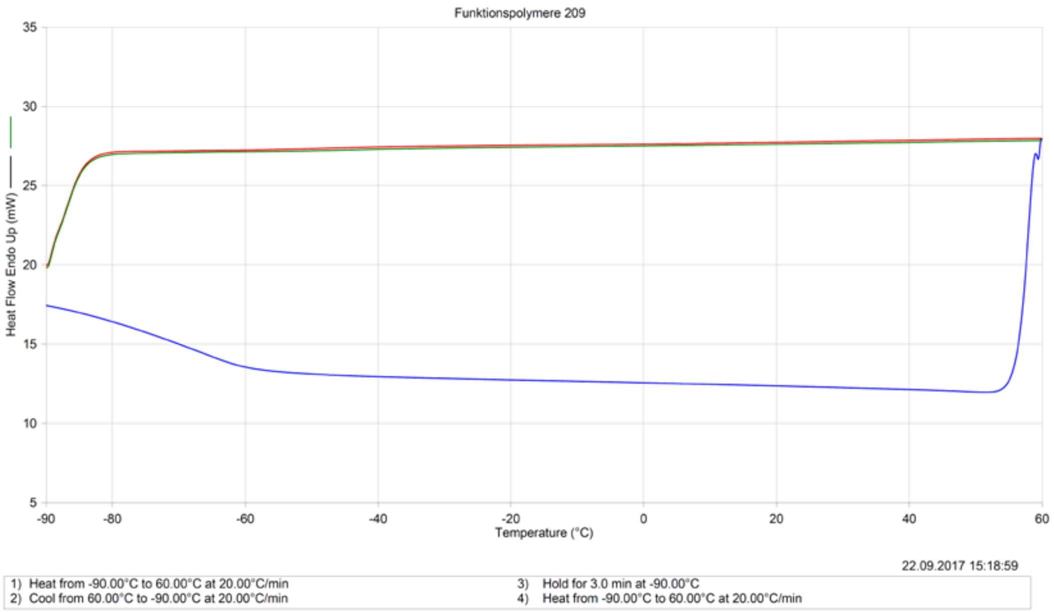

Figure S36. DSC curves of **E2-Cl-20.**

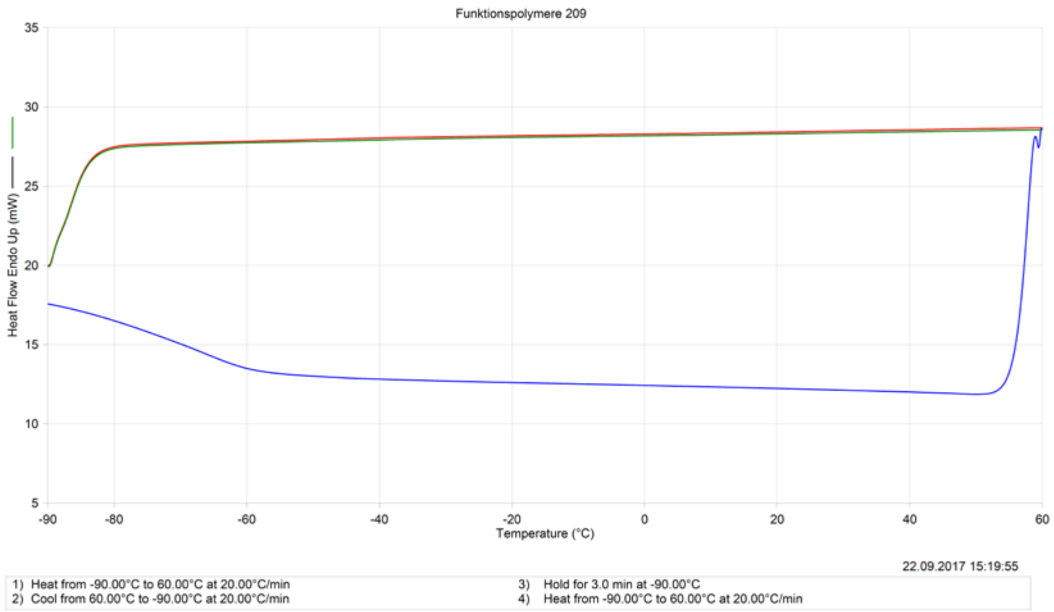

Figure S37. DSC curves of **E2-Cl-33.**

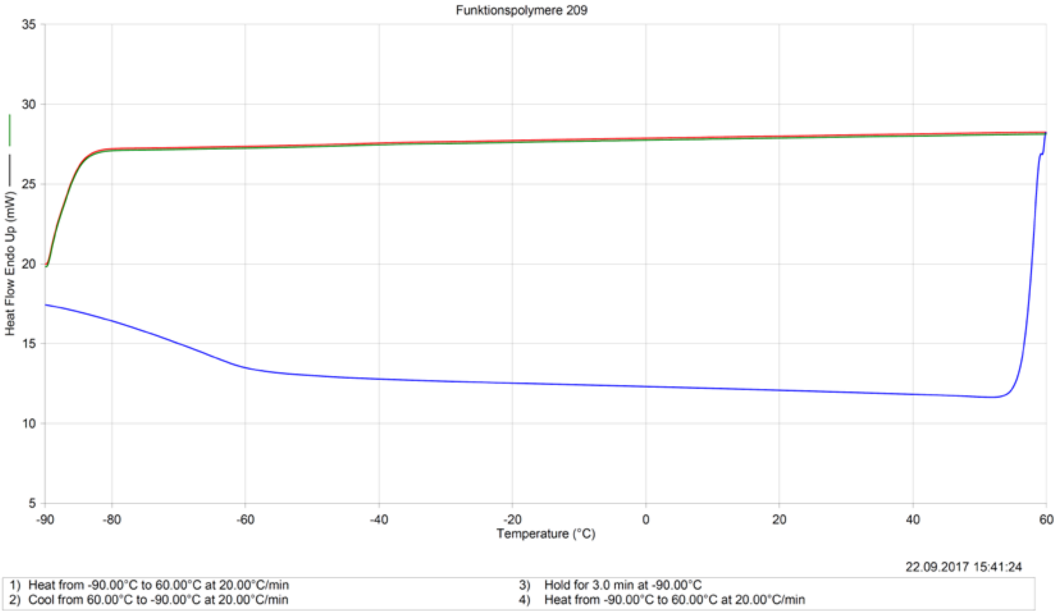

Figure S38. DSC curves of **E2-CN-20.**

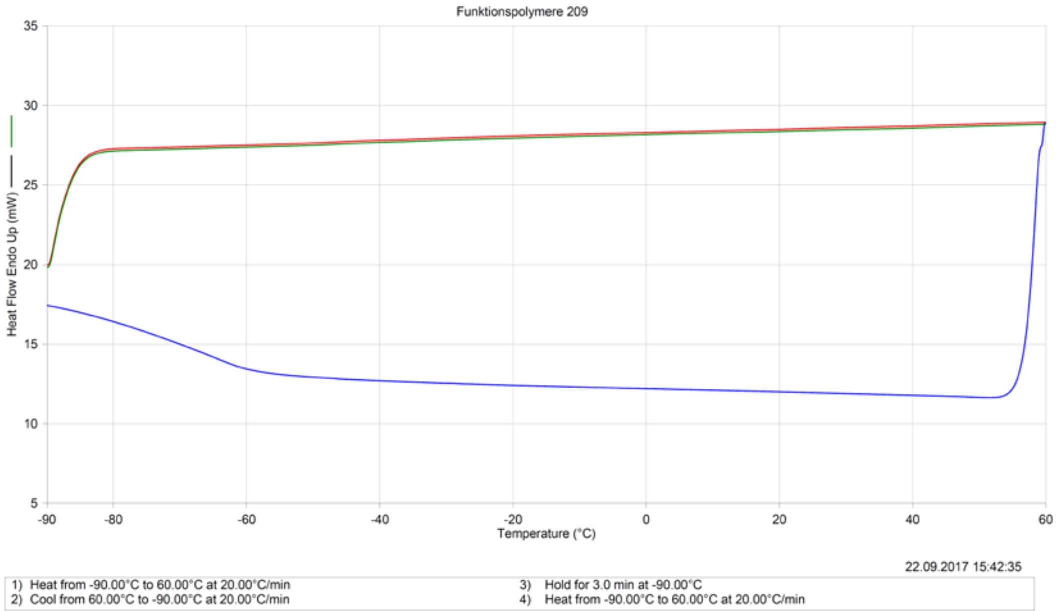

Figure S39. DSC curves of **E2-CN-33.**

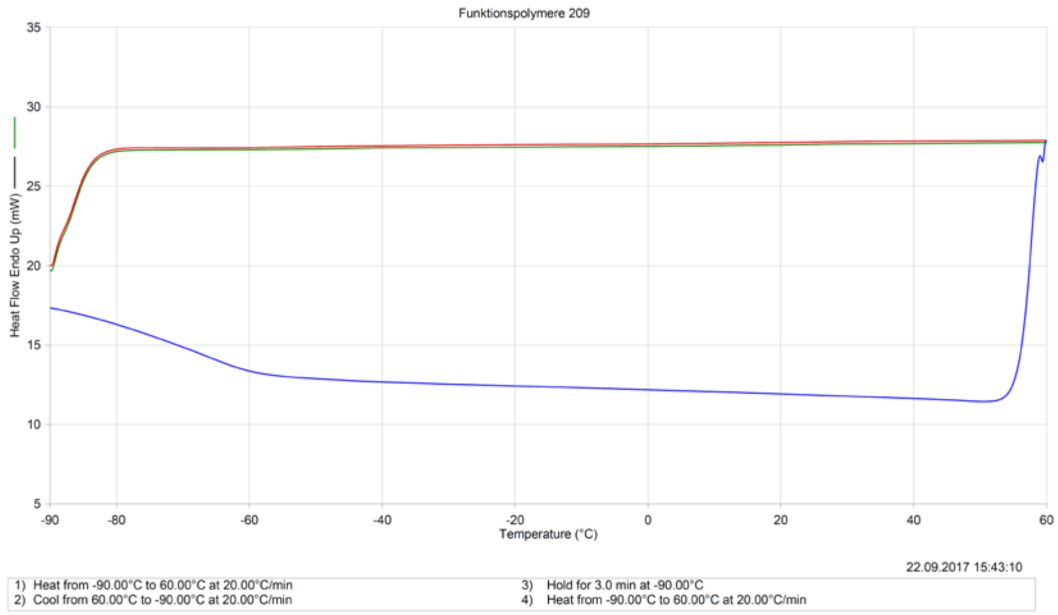

Figure S40. DSC curves of **E3-Cl-20.**

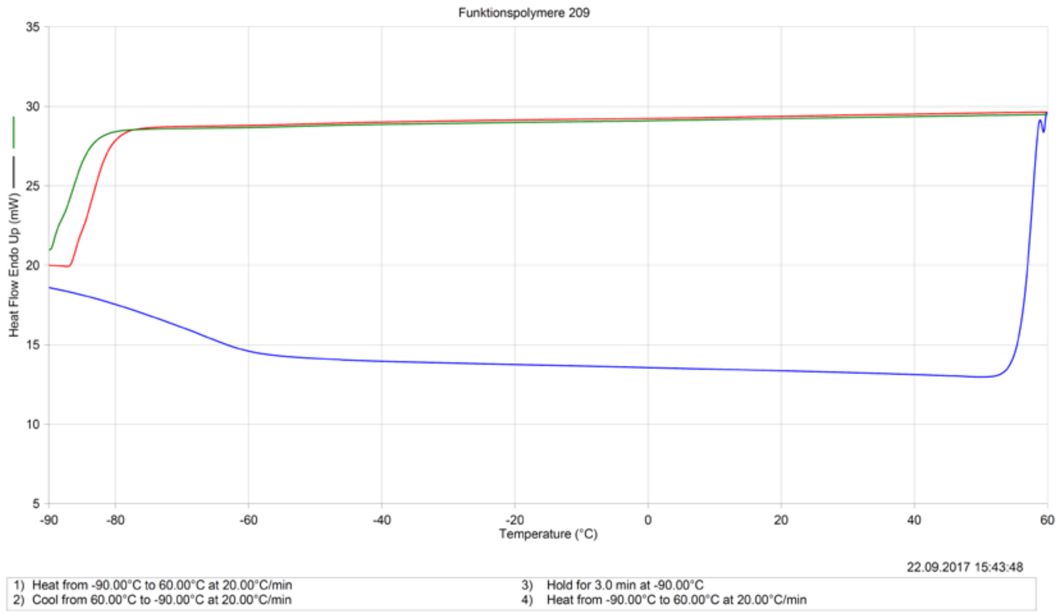

Figure S41. DSC curves of **E3-Cl-33.**

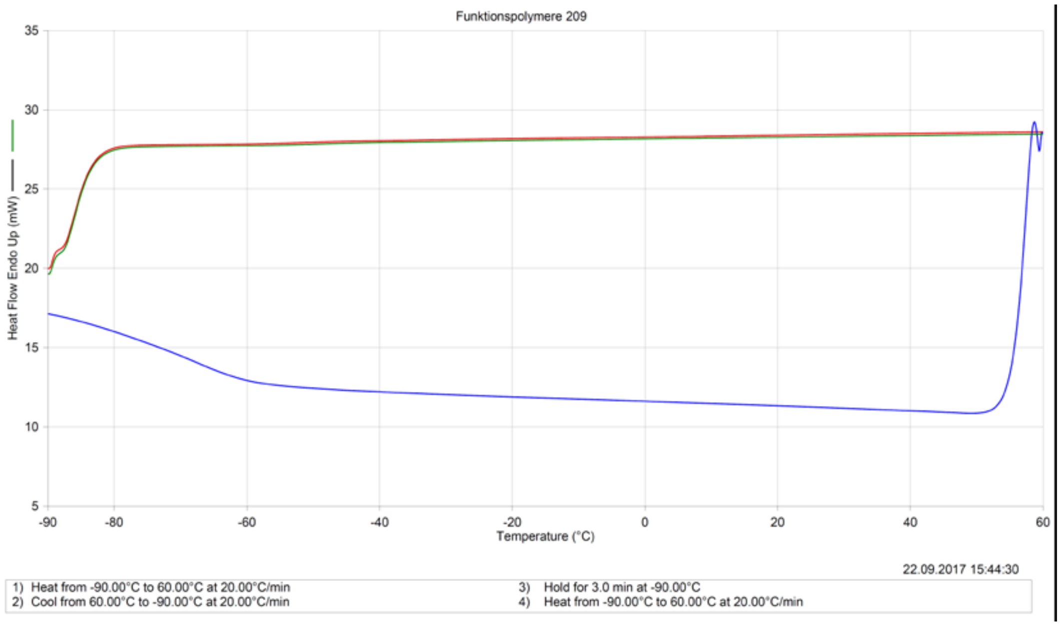

Figure S42. DSC curves of **E3-CN-20.**

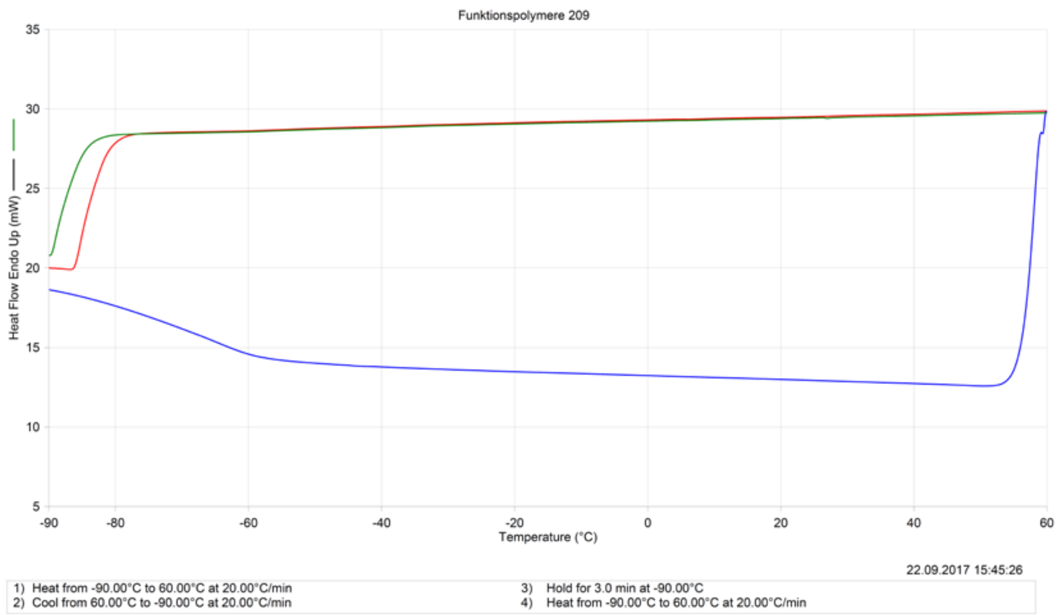

Figure S43. DSC curves of **E3-CN-33**.

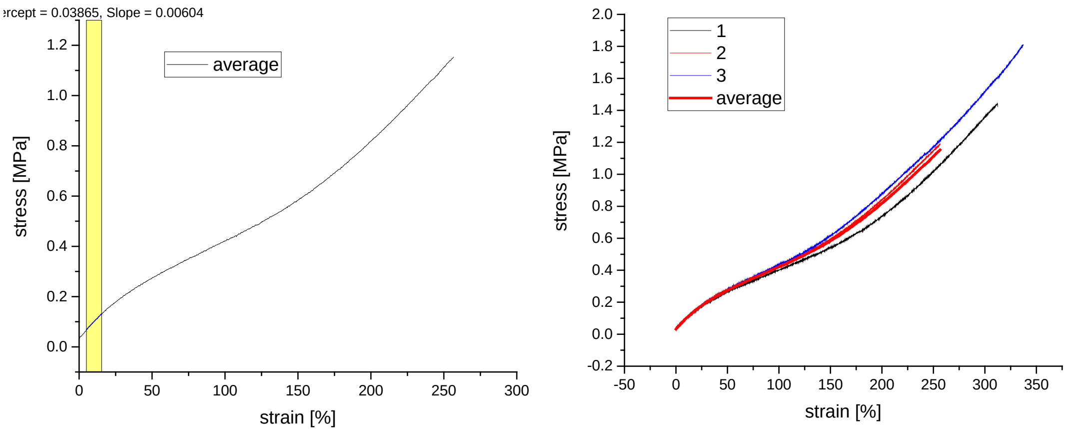

Figure S44. Tensile tests of **Er**. Three independent tests were performed.

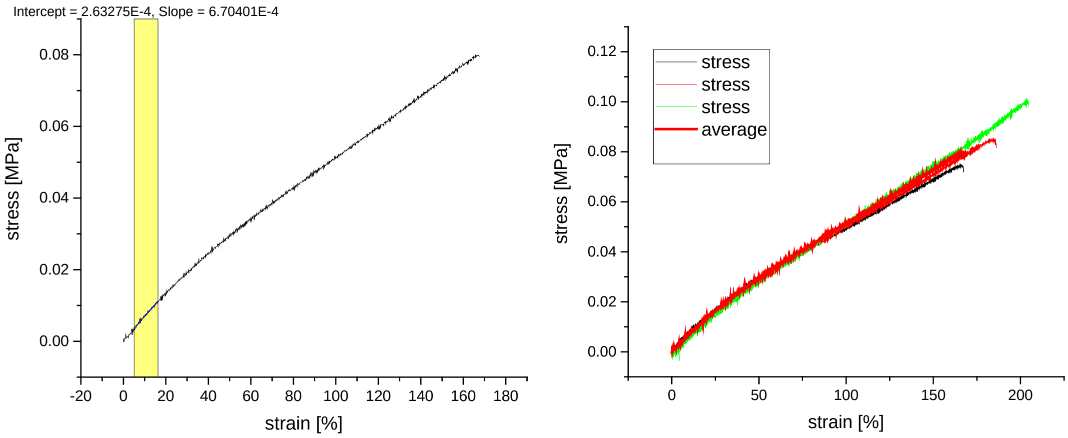

Figure S45. Tensile tests of **E2**. Three independent tests were performed.

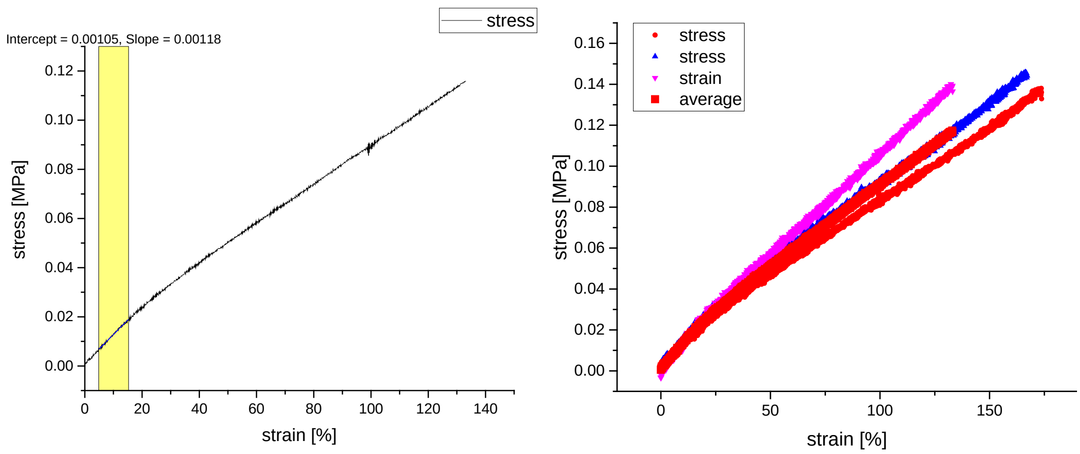

Figure S46. Tensile tests of **E3**. Three independent tests were performed.

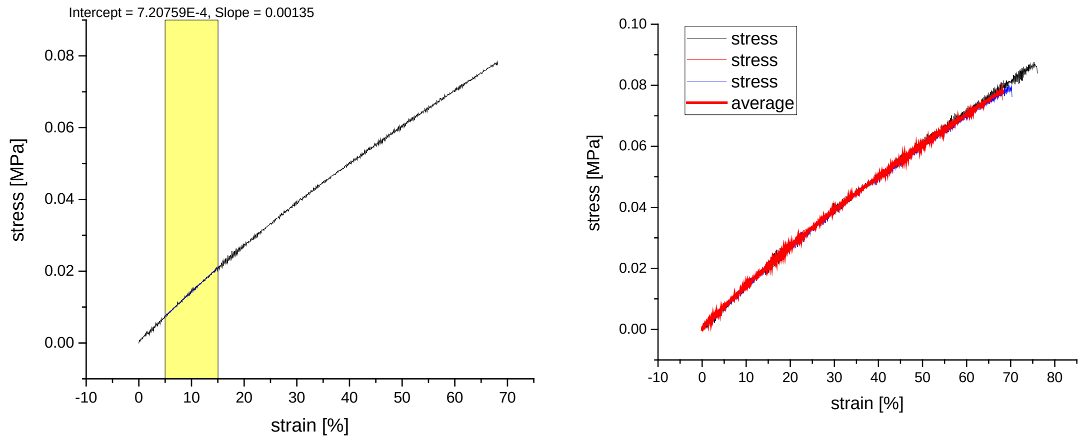

Figure S47. Tensile tests of **E4**. Three independent tests were performed.

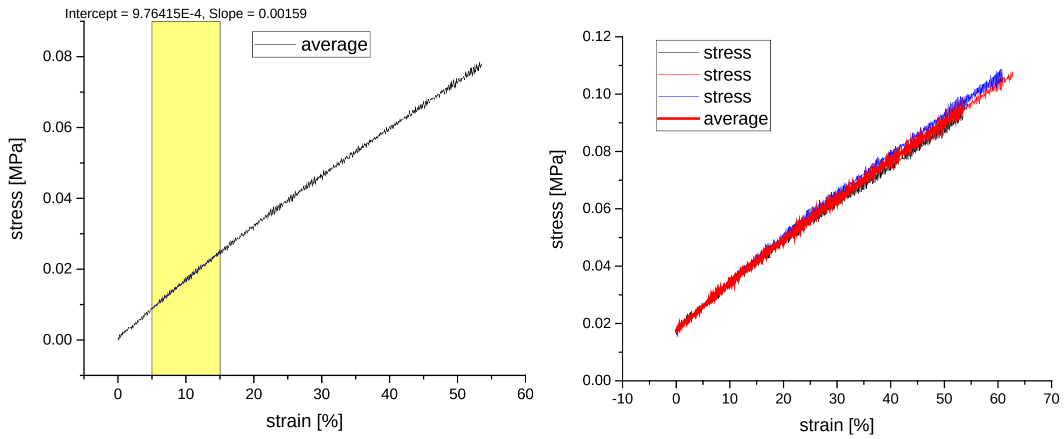

Figure S48. Tensile tests of **E6**. Three independent tests were performed.

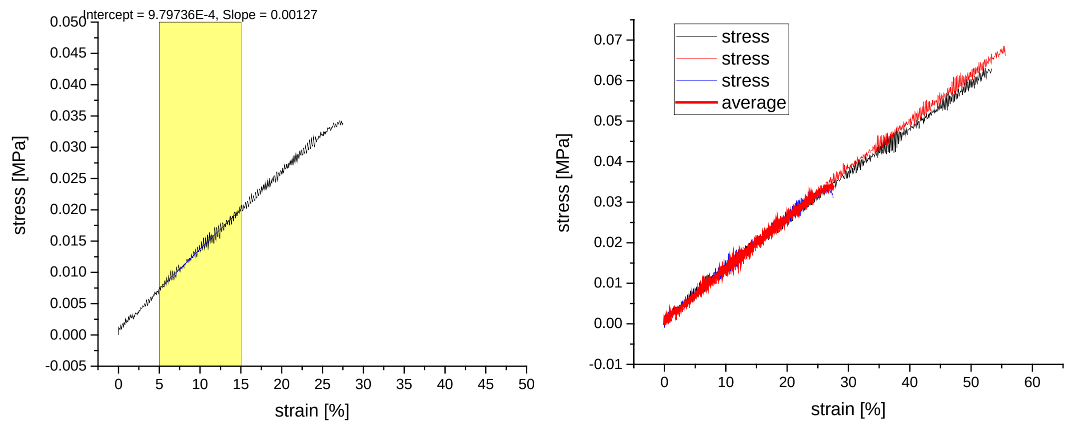

Figure S49. Tensile tests of **E8**. Three independent tests were performed.

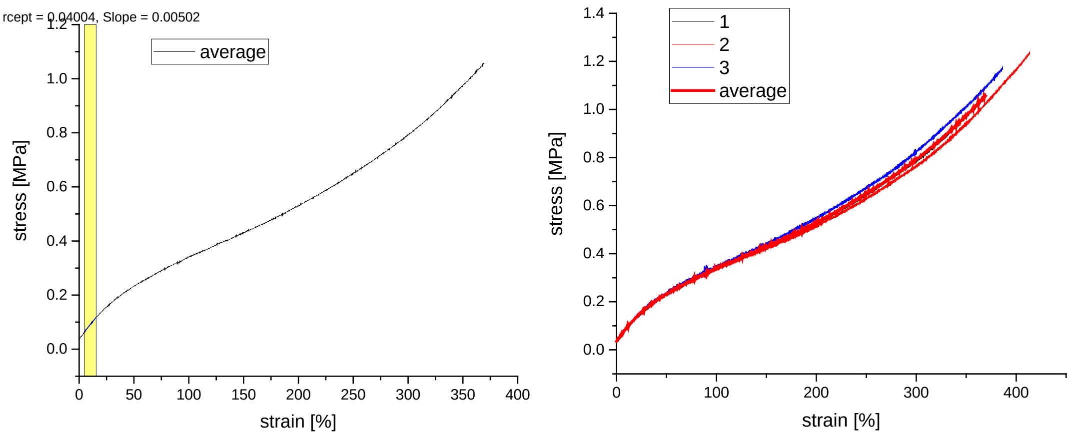

Figure S50. Tensile tests of **Er-Cl-20**. Three independent tests were performed.

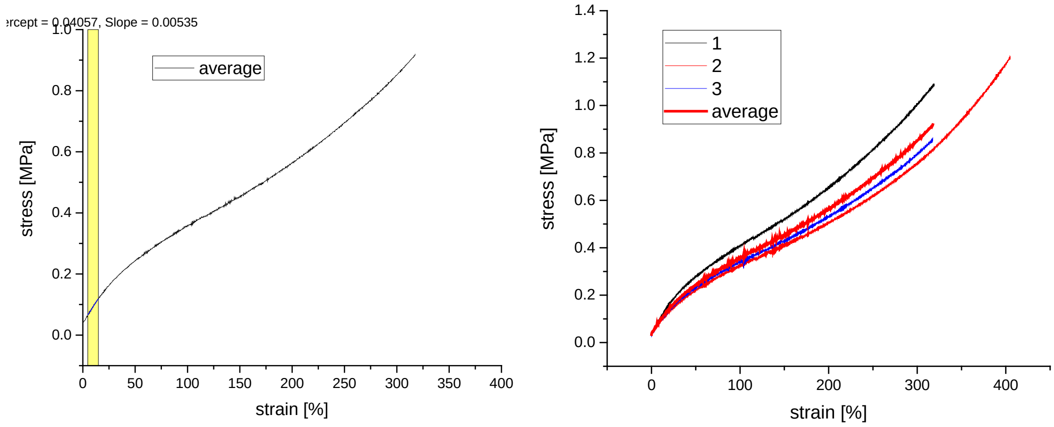

Figure S51. Tensile tests of **Er-Cl-33**. Three independent tests were performed.

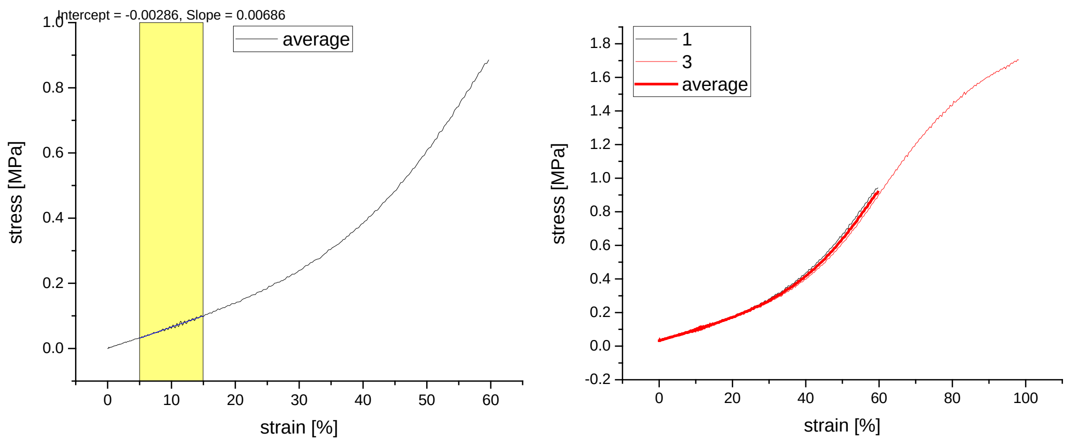

Figure S52. Tensile tests of **E2-Cl-33**. Two independent tests were performed.

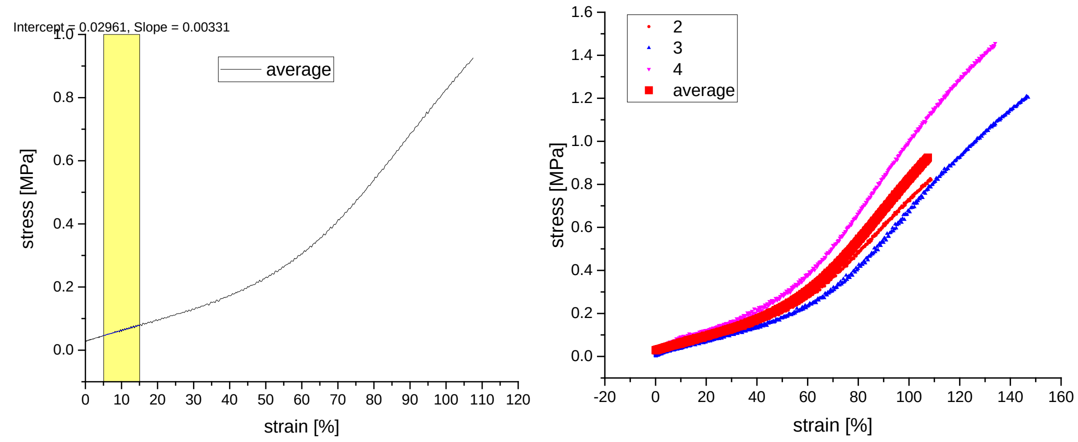

Figure S53. Tensile tests of **E2-Cl-20**. Three independent tests were performed.

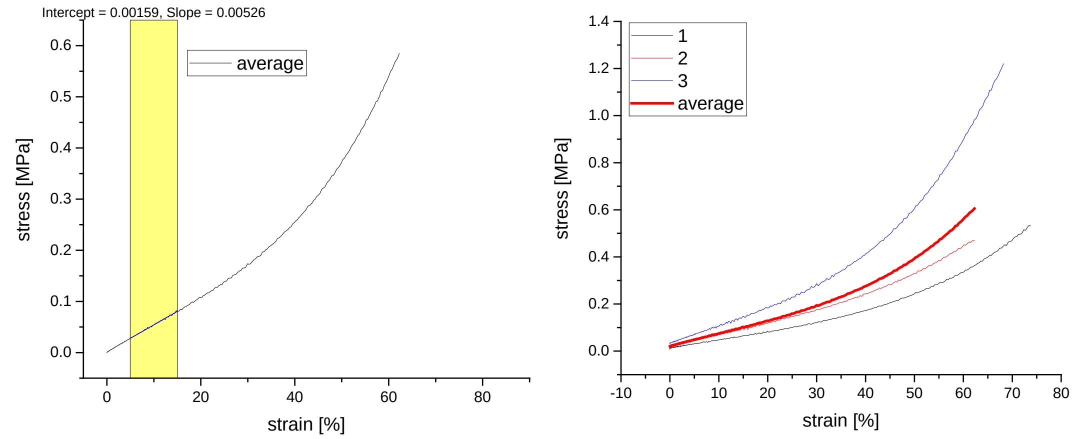

Figure S54. Tensile tests of **E3-Cl-33**. Three independent tests were performed.

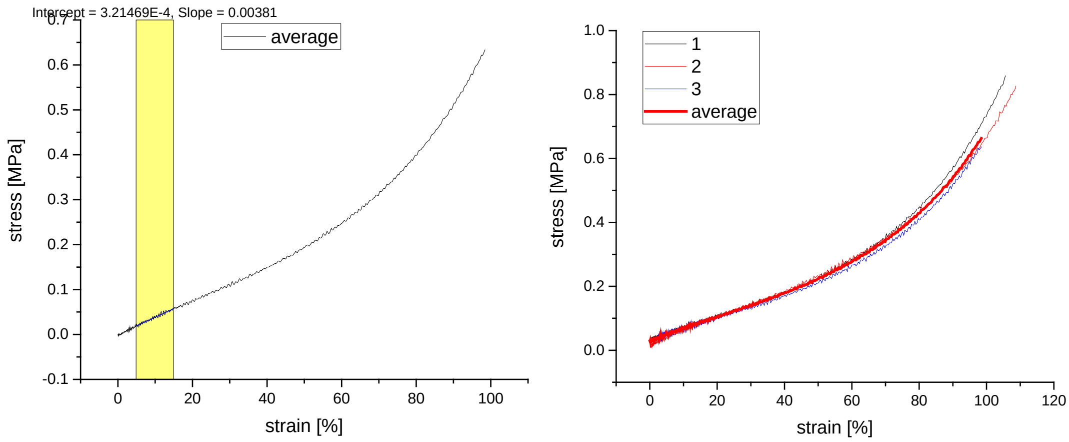

Figure S55. Tensile tests of **E3-Cl-20**. Three independent tests were performed.

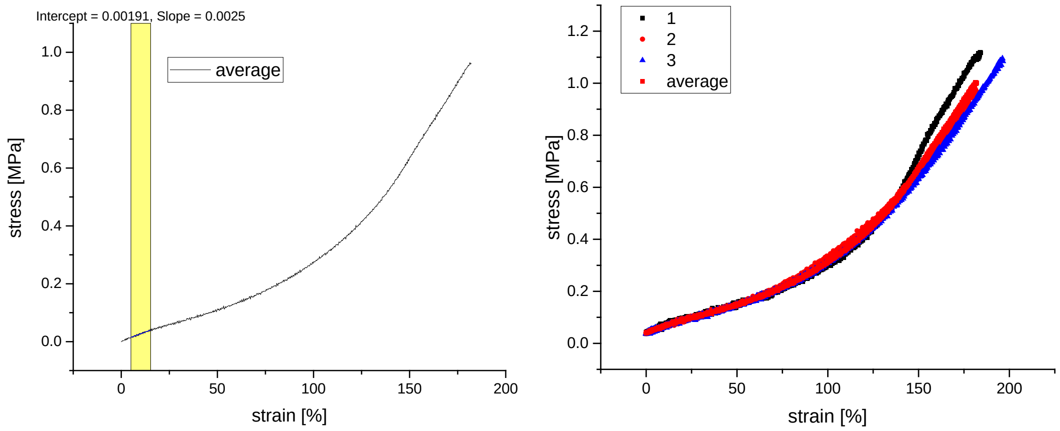

Figure S56. Tensile tests of **E2-CN-33**. Three independent tests were performed.

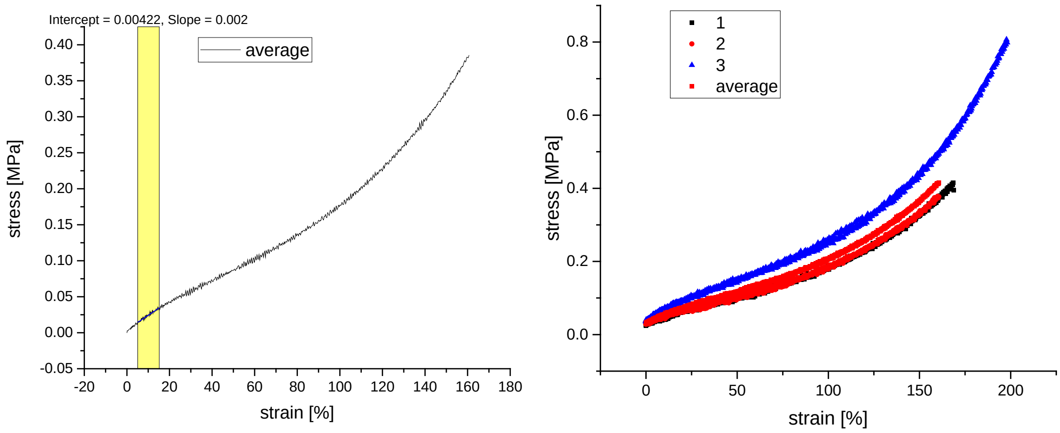

Figure S57. Tensile tests of **E2-CN-20**. Three independent tests were performed.

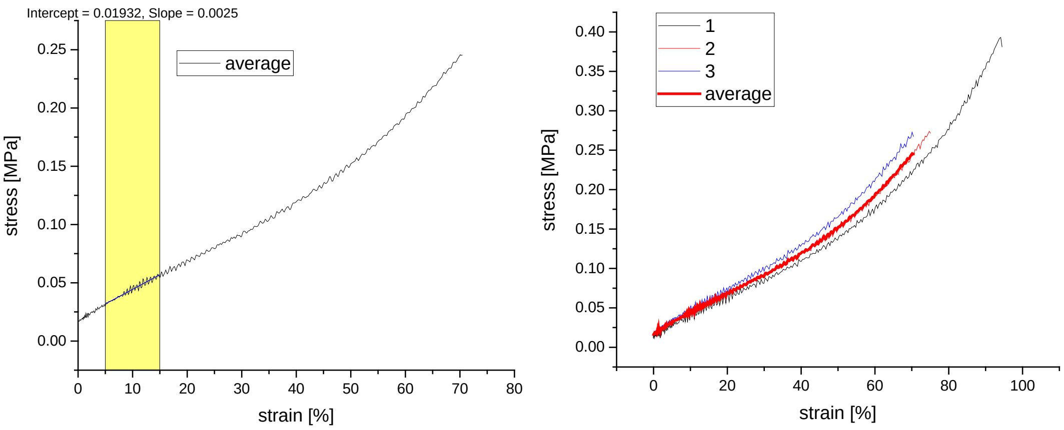

Figure S58. Tensile tests of **E3-CN-33**. Three independent tests were performed.

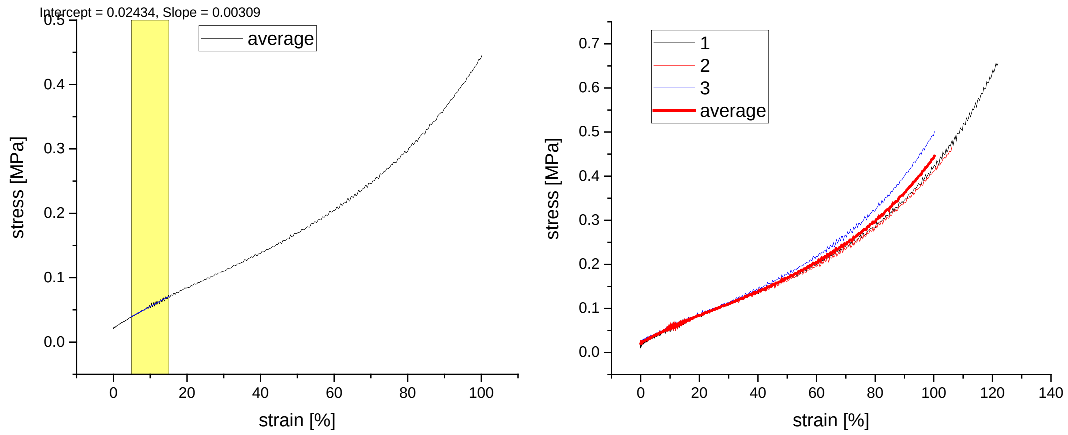

Figure S59. Tensile tests of **E3-CN-20**. Three independent tests were performed.

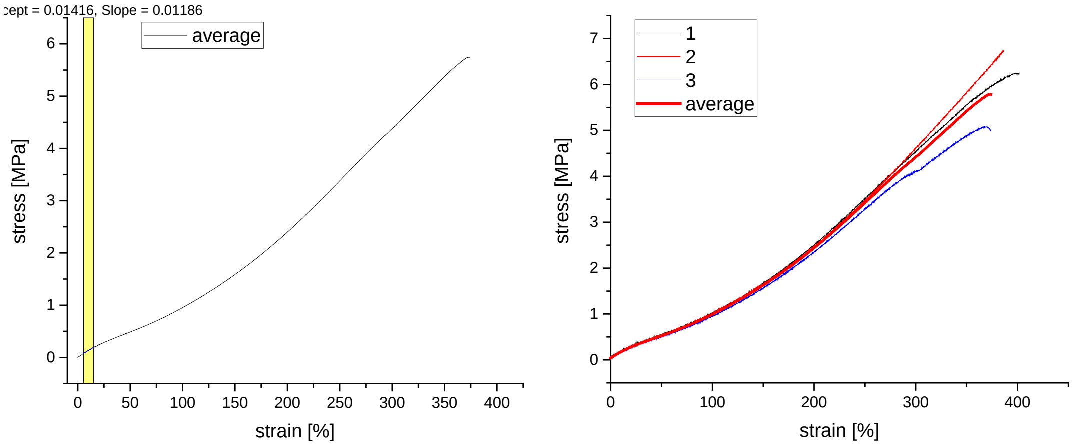

Figure S60. Tensile tests of **Elastosil®Film**. Three independent tests were performed.

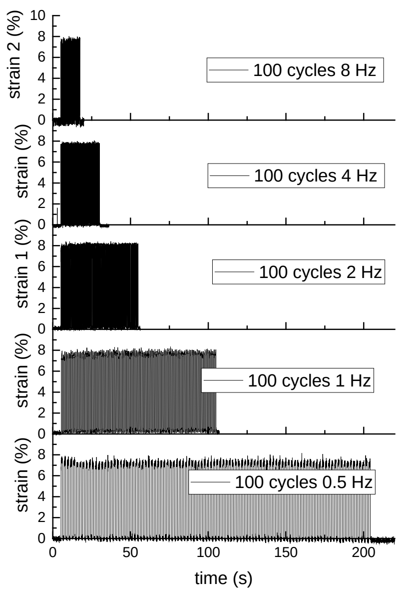

Figure S61. Lateral actuation strain of **Elastosil®Film** 30% prestrained measured at various frequencies (0.5-8 Hz) and an electric field of 90 V μm^{-1}.

Figure S62. Photos showing that the actuator inflates in both directions.

Video 1. Circular membrane actuator constructed from **E3-Cl-20** operated for 100 cycles with 53 V μm^{-1} at 0.5 Hz. The diameter of the film is 25 mm, the electrode diameter is 8 mm. Carbon black powder was used as electrode.

Video 2. Circular membrane actuator constructed from **E3-Cl-20** operated for 1000 cycles at 42 V μm^{-1} at 10 Hz.

Video 3. Circular membrane actuator constructed from **E3-Cl-20** tested at different voltages. The movie was constructed by combining photos which were taken at certain time intervals.